SiG Meeting, Houston, TX, USA

New Developments for the Simulation of Galvanic and Induction Logging Measurements in Deviated and Eccentric Wells

D. Pardo, M. J. Nam, C. Torres-Verdín, M. Paszynski

June 24, 2008

Department of Petroleum and Geosystems Engineering

THE UNIVERSITY OF TEXAS AT AUSTIN

GEOPHYSICAL RESISTIVITY APPLICATIONS

Type of Problems We Can Solve with our FE Software

Applications	Borehole Logging	Controlled Source EM	
Spatial Dimensions	2D	3D	
Well Type	Vertical Well	Deviated Well	Eccentered Well
Logging Instruments	LWD/MWD	Normal/Laterolog	Dual Laterolog
	Triaxial Induction	Dielectric Instruments	Cross-Well
Frequency	0-1 GHz		
Materials	Isotropic	Anisotropic	
Physical Devices	Magnetic Buffers	Insulators	Casing
	Casing Imperfections	Displacement Currents	Combination of All
Sources	Finite Size Antennas	Dipoles in Any Direction	Electrodes
	Solenoidal Antennas	Toroidal Antennas	Combination of All
Invasion	Water	Oil	etc.

MOST (OIL-INDUSTRY) GEOPHYSICAL PROBLEMS

OVERVIEW

1. **Motivation:** Simulation of borehole logging measurements.
2. **Method:**
   - Fourier-finite-element formulation in a non-orthogonal system of coordinates.
   - Goal-oriented self-adaptive hp-FE method.
   - Parallel implementation.
   - Iterative solver.
3. **Numerical Simulations:**
   - Galvanic tools: Through-casing, dual laterolog, deviated wells, eccentric wells, anisotropy, etc.
   - Induction tools: LWD, Triaxial induction, deviated wells, borehole rugosity, anisotropy, etc.
4. **Conclusions and future work.**

MOTIVATION (BOREHOLE LOGGING)

Deviated Wells (Forward Problem)

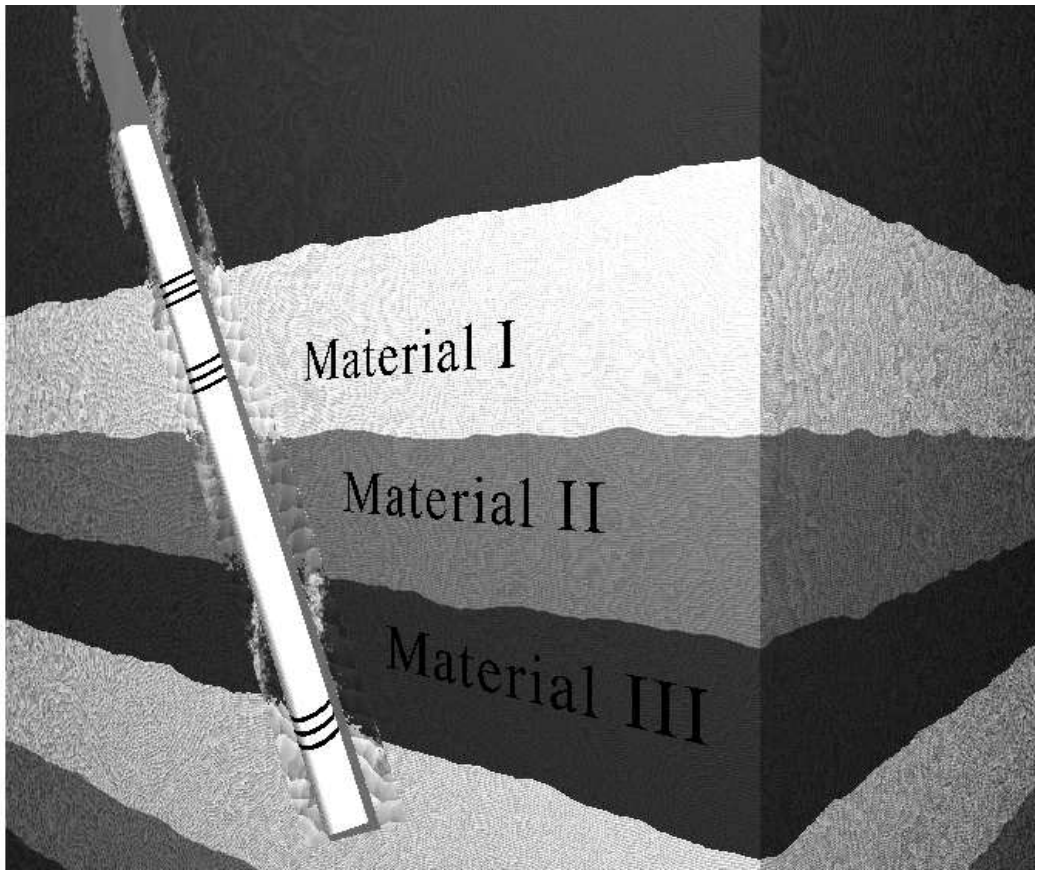

- Dip Angle
- Invasion
- Anisotropy
- Triaxial Induction
- Eccentricity
- Laterolog
- Through-Casing
- Induction-LWD
- Induction-Wireline
- Inverse Problems
- Multi-Physics

Objective: Find solution at the receiver antennas.

MATHEMATICAL FORMULATION (3D)

3D Variational Formulation

Time-Harmonic Maxwell's Equations

$\nabla \times \mathrm{H} = \mathring{\sigma}\mathrm{E} + \mathrm{J}^{imp}$	**Ampere's law ($\mathring{\sigma} = \sigma + j\omega\epsilon$)**
$\nabla \times \mathrm{E} = \mathring{\mu}\mathrm{H} + \mathrm{M}^{imp}$	**Faraday's law ($\mathring{\mu} = -j\omega\mu$)**
$\nabla \cdot (\epsilon \mathrm{E}) = \rho$	**Gauss' law of Electricity**
$\nabla \cdot (\mu \mathrm{H}) = 0$	**Gauss' law of Magnetism**

E-VARIATIONAL FORMULATION:

$$
\begin{cases}
\text{Find } \mathrm{E} \in \mathrm{E}_{\Gamma_E} + \boldsymbol{H}_{\Gamma_E}(\mathrm{curl};\Omega) \text{ such that:} \\
\left\langle \nabla \times \mathrm{F}, \mathring{\mu}^{-1} \nabla \times \mathrm{E} \right\rangle_{L^2(\Omega)} - \left\langle \mathrm{F}, \mathring{\sigma}\mathrm{E} \right\rangle_{L^2(\Omega)} = \left\langle \mathrm{F}, \mathrm{J}^{imp} \right\rangle_{L^2(\Omega)} \\
- \left\langle \mathrm{F}_t, \mathrm{J}^{imp}_{\Gamma_H} \right\rangle_{L^2(\Gamma_H)} + \left\langle \nabla \times \mathrm{F}, \mathring{\mu}^{-1} \mathrm{M}^{imp} \right\rangle_{L^2(\Omega)} \quad \forall\, \mathrm{F} \in \boldsymbol{H}_{\Gamma_E}(\mathrm{curl};\Omega)
\end{cases}
$$

FOURIER ANALYSIS

Dimensionality Reduction for Maxwell's Equations

Solving a 3D problem is CPU time and memory intensive. In some cases, we may reduce the complexity of the problem by using Fourier analysis.

Borehole Problems

Cylindrical Coordinates

Fourier Series Expansion

$$\mathrm{E}(\phi) := \frac{1}{\sqrt{2\pi}} \sum_{n=-\infty}^{\infty} \mathcal{F}_n(\mathrm{E}) e^{jn\phi}$$

X-Well, CSEM Problems

Cartesian Coordinates

Fourier Transform

$$\mathrm{E}(x_1) := \frac{1}{\sqrt{2\pi}} \int_{\mathbb{R}} \mathcal{F}_r(\mathrm{E}) e^{jrx_1} dx_1$$

FOURIER ANALYSIS

Fourier Series Expansion

Fourier series expansion **Inverse Fourier series expansion**

$$\mathcal{F}_n(\mathrm{E}) := \frac{1}{\sqrt{2\pi}} \int_0^{2\pi} \mathrm{E}(\phi) e^{-jn\phi} d\phi \quad ; \quad \mathrm{E}(\phi) = \frac{1}{\sqrt{2\pi}} \sum_{n=-\infty}^{\infty} \mathcal{F}_n(\mathrm{E}) e^{jn\phi}.$$

Main properties

- **Compatibility with differentiation** $\mathcal{F}_n(\frac{\partial \mathrm{E}}{\partial \phi}) = jn\mathcal{F}_n(\mathrm{E})$**:**

$$\mathcal{F}_n(\nabla \times \mathrm{E}) = \nabla^n \times (\mathcal{F}_n(\mathrm{E})),$$

where

$$\nabla^n \times \mathrm{E} := \left(\frac{jnE_z}{\rho} - \frac{\partial E_\phi}{\partial z}, \frac{\partial E_\rho}{\partial z} - \frac{\partial E_z}{\partial \rho}, \frac{1}{\rho} \frac{\partial (\rho E_\phi)}{\partial \rho} - \frac{jnE_\rho}{\rho} \right),$$

- L_2**-Orthogonality:**

$$\frac{1}{\sqrt{2\pi}} \int_0^{2\pi} e^{jn\phi} e^{-jm\phi} d\phi = \sqrt{2\pi} \delta_{nm} \, .$$

FOURIER ANALYSIS

Fourier Transform

Fourier transform **Inverse Fourier transform**

$$\mathcal{F}_r(\mathbf{E}) := \frac{1}{\sqrt{2\pi}} \int_{\mathbb{R}} \mathbf{E}(x) e^{-jrx} dx \quad ; \quad \mathbf{E}(x) = \frac{1}{\sqrt{2\pi}} \int_{\mathbb{R}} \mathcal{F}_r(\mathbf{E}) e^{jrx} dr.$$

Main properties

- **Compatibility with differentiation** $\mathcal{F}_r(\frac{\partial \mathbf{E}}{\partial x}) = jr\mathcal{F}_r(\mathbf{E})$**:**

$$\mathcal{F}_r(\nabla \times \mathbf{E}) = \nabla^r \times (\mathcal{F}_r(\mathbf{E})),$$

where

$$\nabla^r \times \mathbf{E} := \left(\frac{\partial E_z}{\partial y} - \frac{\partial E_y}{\partial z}, \frac{\partial E_x}{\partial z} - jrE_z, jrE_y - \frac{\partial E_x}{\partial y} \right),$$

- L_2**-Orthogonality:**

$$\frac{1}{\sqrt{2\pi}} \int_{\mathbb{R}} e^{jrx} e^{-jsx} = \sqrt{2\pi}\delta_{sr} \ .$$

FOURIER ANALYSIS

E-Variational Formulations (Cylindrical Coordinates)

FINITE ELEMENT —3D—:

$$
\begin{cases}
\text{Find } \mathbf{E} \in \mathbf{E}_{\Gamma_E} + H_{\Gamma_E}(\mathrm{curl};\Omega) \text{ such that:} \\
\left\langle \nabla \times \mathbf{F}, \mathring{\mu}^{-1} \nabla \times \mathbf{E} \right\rangle_{L^2(\Omega)} - \left\langle \mathbf{F}, \mathring{\sigma} \mathbf{E} \right\rangle_{L^2(\Omega)} = \left\langle \mathbf{F}, \mathbf{J}^{imp} \right\rangle_{L^2(\Omega)} \\
- \left\langle \mathbf{F}_t, \mathbf{J}^{imp}_{\Gamma_H} \right\rangle_{L^2(\Gamma_H)} + \left\langle \nabla \times \mathbf{F}, \mathring{\mu}^{-1} \mathbf{M}^{imp} \right\rangle_{L^2(\Omega)} \quad \forall\, \mathbf{F} \in H_{\Gamma_E}(\mathrm{curl};\Omega)
\end{cases}
$$

FOURIER FINITE ELEMENT —3D = Sequence of Coupled 2D Problems—:

$$
\begin{cases}
\text{Find } \mathbf{E} = \dfrac{1}{\sqrt{2\pi}} \displaystyle\sum_{n=-\infty}^{\infty} \mathcal{F}_n(\mathbf{E})\, e^{jn\phi}, \text{ where for each } n: \\
\mathcal{F}_n(\mathbf{E}) \in \mathcal{F}_n(\mathbf{E}_{\Gamma_{E,1D}}) + H_{\Gamma_{E,1D}}(\mathrm{curl}^n;\Omega_{2D}), \text{ and} \\
\displaystyle\sum_{m=-\infty}^{\infty} \left\langle \nabla^n \times \mathcal{F}_n(\mathbf{F}) \,,\, \mathcal{F}_{n-m}(\mathring{\mu}^{-1}) \nabla^m \times \mathcal{F}_m(\mathbf{E}) \right\rangle_{L^2(\Omega_{2D})} - \left\langle \mathcal{F}_n(\mathbf{F}) \,,\, \mathcal{F}_{n-m}(\mathring{\sigma}) \mathcal{F}_m(\mathbf{E}) \right\rangle_{L^2(\Omega_{2D})} \\
= \left\langle \mathcal{F}_n(\mathbf{F}) \,,\, \mathcal{F}_n(\mathbf{J}^{imp}) \right\rangle_{L^2(\Omega_{2D})} - \left\langle \mathcal{F}_n(\mathbf{F}_t) \,,\, \mathcal{F}_n(\mathbf{J}^{imp}_S) \right\rangle_{L^2(\Gamma_{H,1D})} \\
+ \displaystyle\sum_{m=-\infty}^{\infty} \left\langle \nabla^n \times \mathcal{F}_n(\mathbf{F}) \,,\, \mathcal{F}_{n-m}(\mathring{\mu}^{-1}) \mathcal{F}_m(\mathbf{M}^{imp}) \right\rangle_{L^2(\Omega_{2D})} \quad \forall\, \mathcal{F}_n(\mathbf{F}) \in H_{\Gamma_{E,1D}}(\mathrm{curl}^n;\Omega_{2D})
\end{cases}
$$

FOURIER ANALYSIS

Cartesian system of coordinates: $\mathrm{x} = (x, y, z)$.

New non-orthogonal system of coordinates: $\zeta = (\zeta_1, \zeta_2, \zeta_3)$.

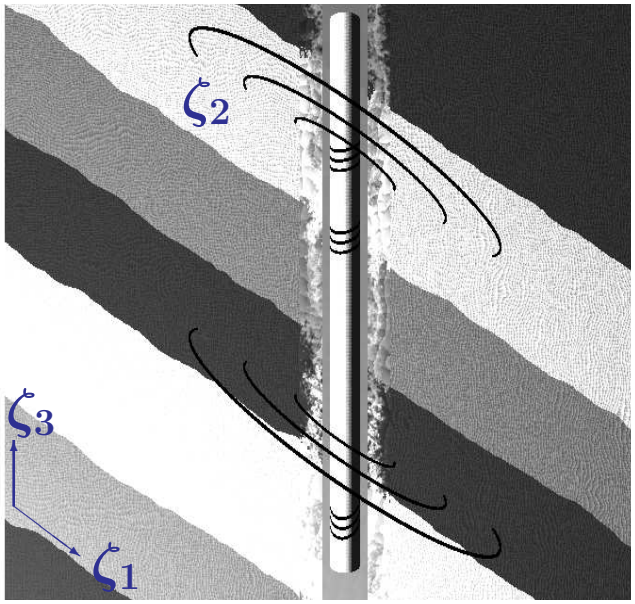

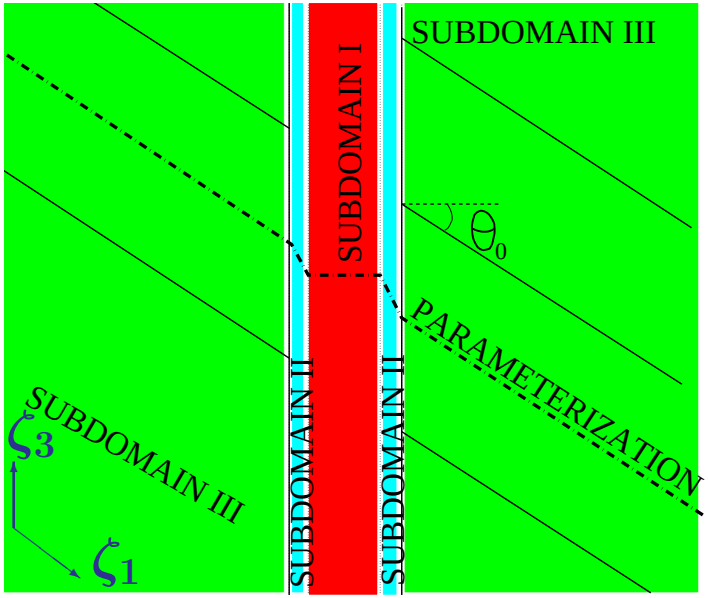

Subdomain I ; **Subdomain II** ; **Subdomain III**

$$\begin{cases} x = \zeta_1 \cos\zeta_2 \\ y = \zeta_1 \sin\zeta_2 \\ z = \zeta_3 \end{cases} ; \quad \begin{cases} x = \zeta_1 \cos\zeta_2 \\ y = \zeta_1 \sin\zeta_2 \\ z = \zeta_3 + \tan\theta_0 \dfrac{\zeta_1 - \rho_1}{\rho_2 - \rho_1}\rho_2 \end{cases} ; \quad \begin{cases} x = \zeta_1 \cos\zeta_2 \\ y = \zeta_1 \sin\zeta_2 \\ z = \zeta_3 + \tan\theta_0 \zeta_1 \end{cases}$$

FOURIER ANALYSIS

E-Variational Formulation in the New System of Coordinates ζ

In the new system of coordinates, we obtain:

3D FOURIER FINITE ELEMENT FORMULATION
— Sequence of "Weakly" Coupled 2D Problems —

$$
\left\{
\begin{array}{l}
\text{Find } \mathbf{E} = \dfrac{1}{\sqrt{2\pi}} \displaystyle\sum_{n=-\infty}^{\infty} \mathcal{F}_n(\mathbf{E})\, e^{jn\zeta_2}, \text{ where for each } n\text{:} \\
\mathcal{F}_n(\mathbf{E}) \in \mathcal{F}_n(\mathbf{E}_{\Gamma_{E,1D}}) + H_{\Gamma_{E,1D}}(\mathbf{curl}^n;\Omega_{2D}), \text{ and} \\
\displaystyle\sum_{m=-2}^{2} \left\langle \nabla^n \times \mathcal{F}_n(\mathbf{F}) \,,\, \mathcal{F}_{n-m}(\mathring{\mu}_{mod}^{-1}) \nabla^m \times \mathcal{F}_m(\mathbf{E}) \right\rangle_{L^2(\Omega_{2D})} - \left\langle \mathcal{F}_n(\mathbf{F}) \,,\, \mathcal{F}_{n-m}(\mathring{\sigma}_{mod}) \mathcal{F}_m(\mathbf{E}) \right\rangle_{L^2(\Omega_{2D})} \\
\quad = \left\langle \mathcal{F}_n(\mathbf{F}) \,,\, \mathcal{F}_n(\mathbf{J}^{imp}) \right\rangle_{L^2(\Omega_{2D})} - \left\langle \mathcal{F}_n(\mathbf{F}_t) \,,\, \mathcal{F}_n(\mathbf{J}_S^{imp}) \right\rangle_{L^2(\Gamma_{H,1D})} \\
\quad + \displaystyle\sum_{m=-2}^{2} \left\langle \nabla^n \times \mathcal{F}_n(\mathbf{F}) \,,\, \mathcal{F}_{n-m}(\mathring{\mu}_{mod}^{-1}) \mathcal{F}_m(\mathbf{M}^{imp}) \right\rangle_{L^2(\Omega_{2D})} \quad \forall\, \mathcal{F}_n(\mathbf{F}) \in H_{\Gamma_{E,1D}}(\mathbf{curl}^n;\Omega_{2D})
\end{array}
\right.
$$

Five Fourier modes are sufficient to represent EXACTLY the new material coefficients resulting from incorporating the change of coordinates.

FOURIER-FINITE-ELEMENT: ILLUSTRATION

Model Problem

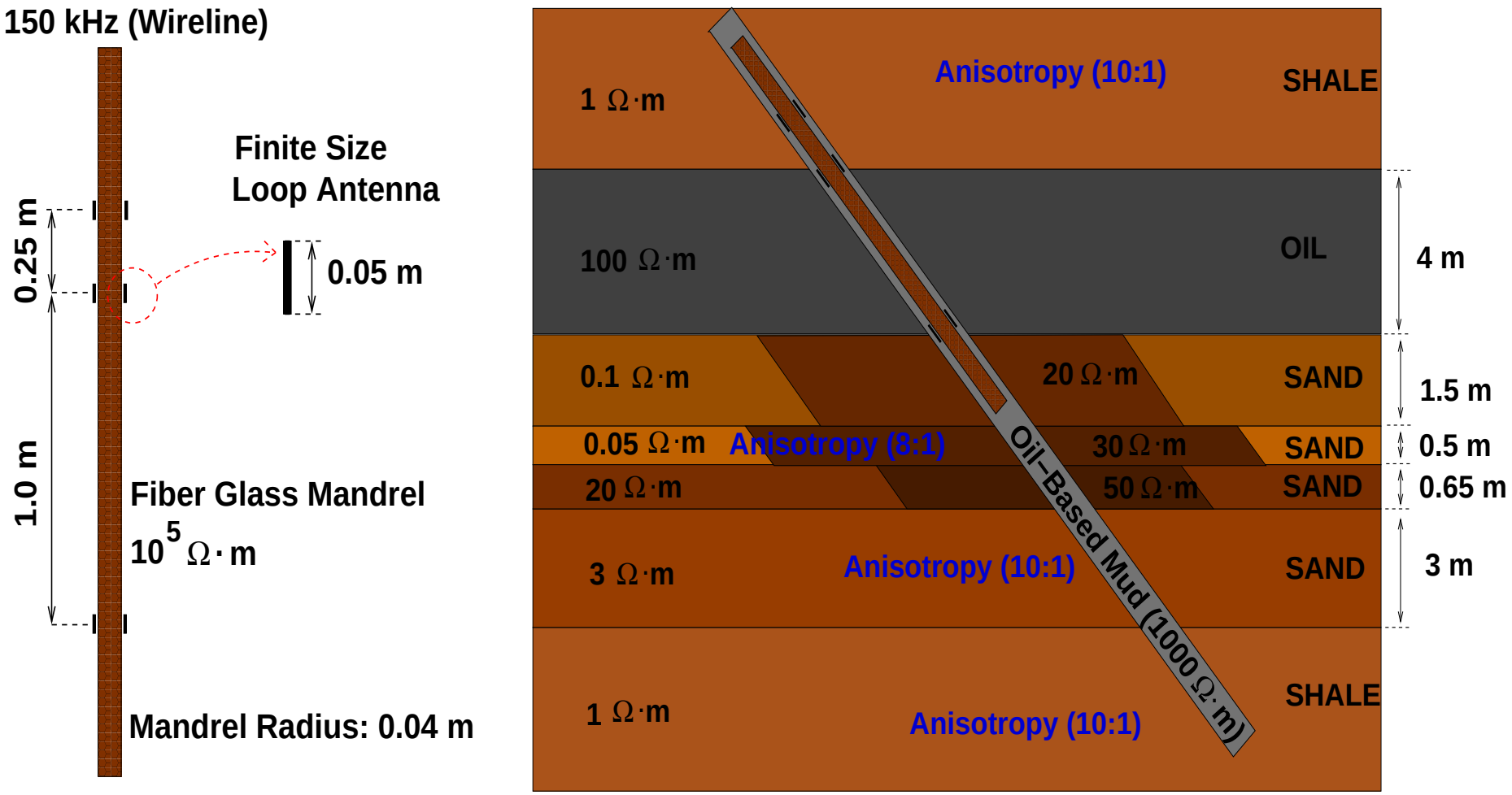

FOURIER-FINITE-ELEMENT: ILLUSTRATION

Verification

Logging Instrument in a Homogeneous Formation

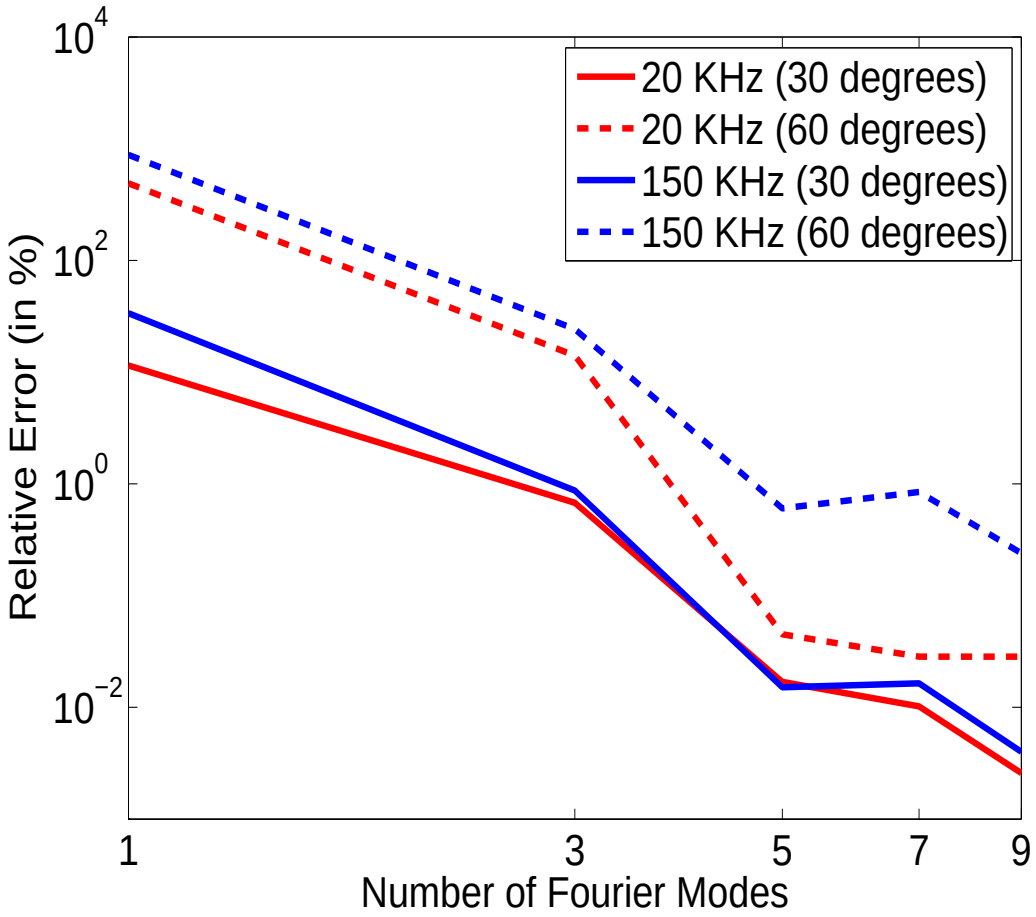

FOURIER-FINITE-ELEMENT: ILLUSTRATION

Verification

Logging Instrument in a Homogeneous Formation

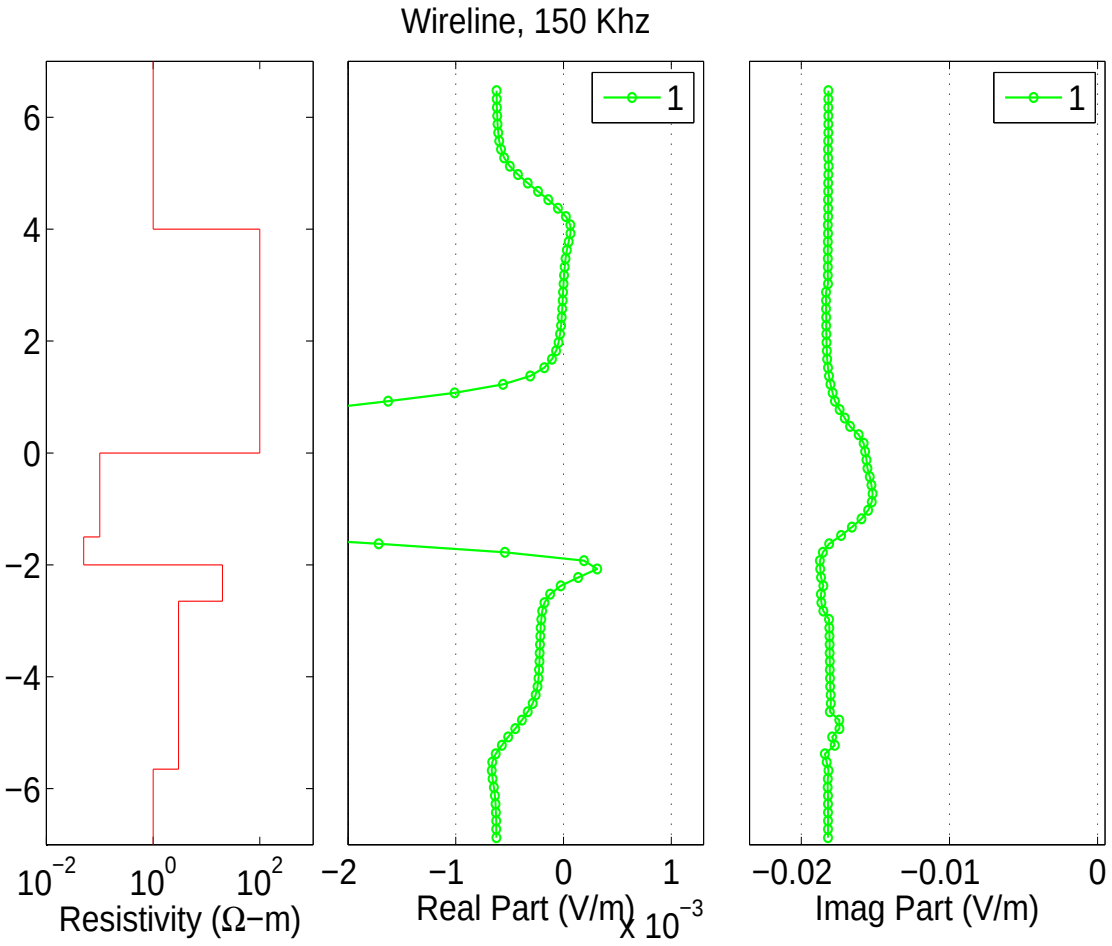

FOURIER-FINITE-ELEMENT: ILLUSTRATION

Verification

Logging Instrument in a Homogeneous Formation

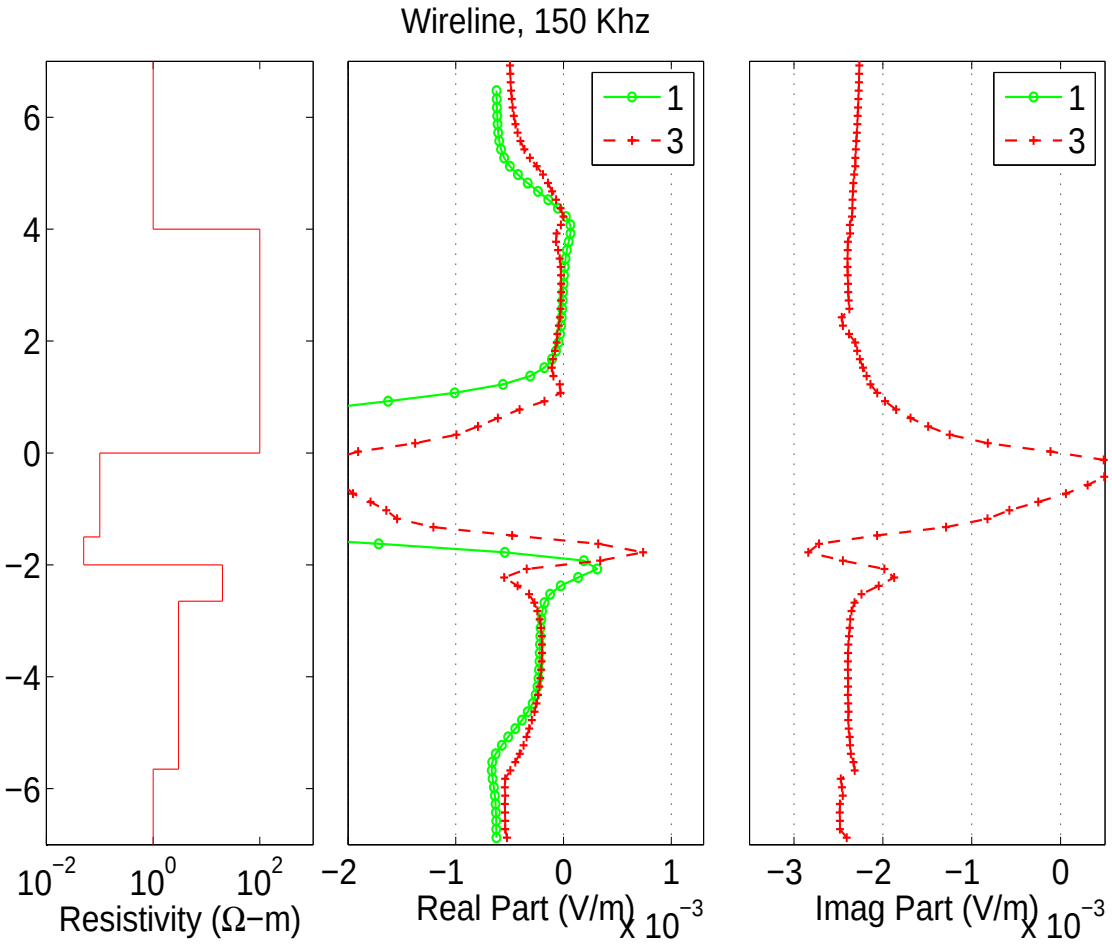

FOURIER-FINITE-ELEMENT: ILLUSTRATION

Verification

Logging Instrument in a Homogeneous Formation

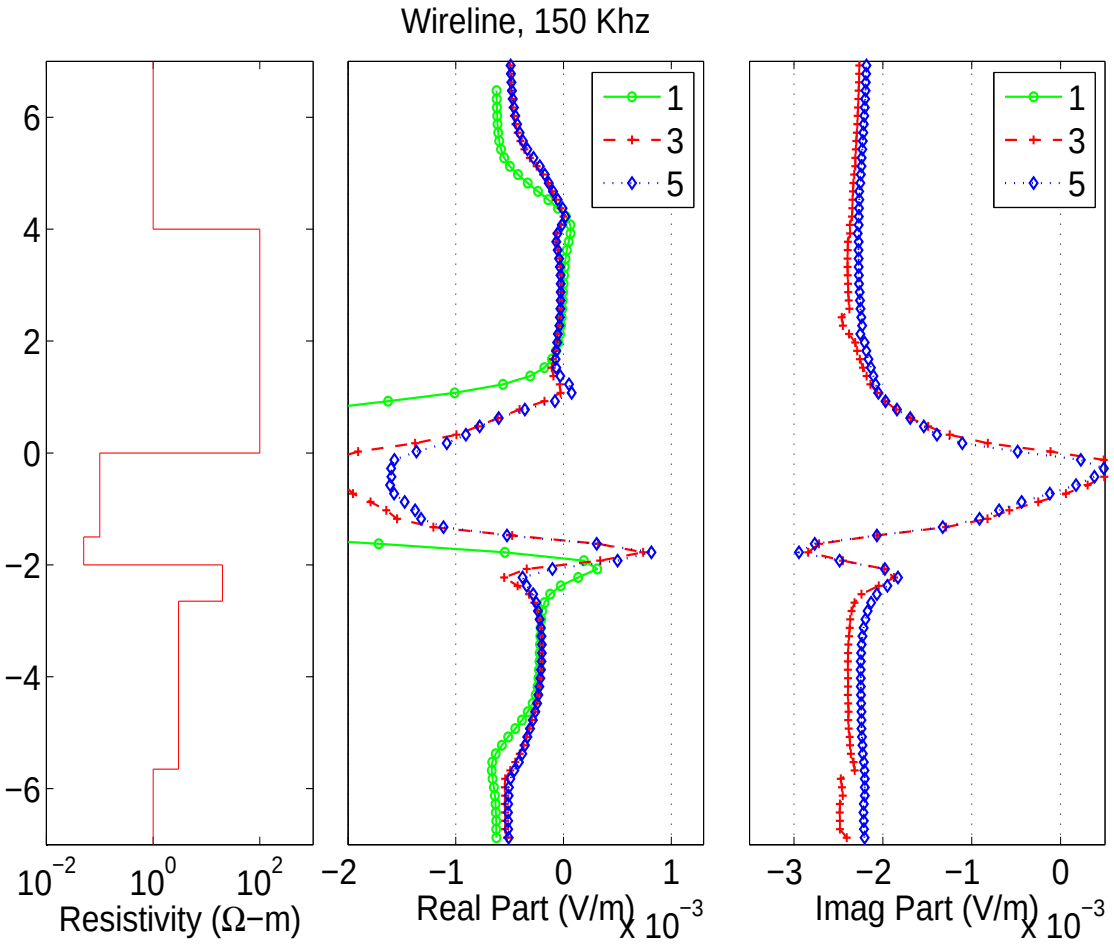

FOURIER-FINITE-ELEMENT: ILLUSTRATION

Verification

Logging Instrument in a Homogeneous Formation

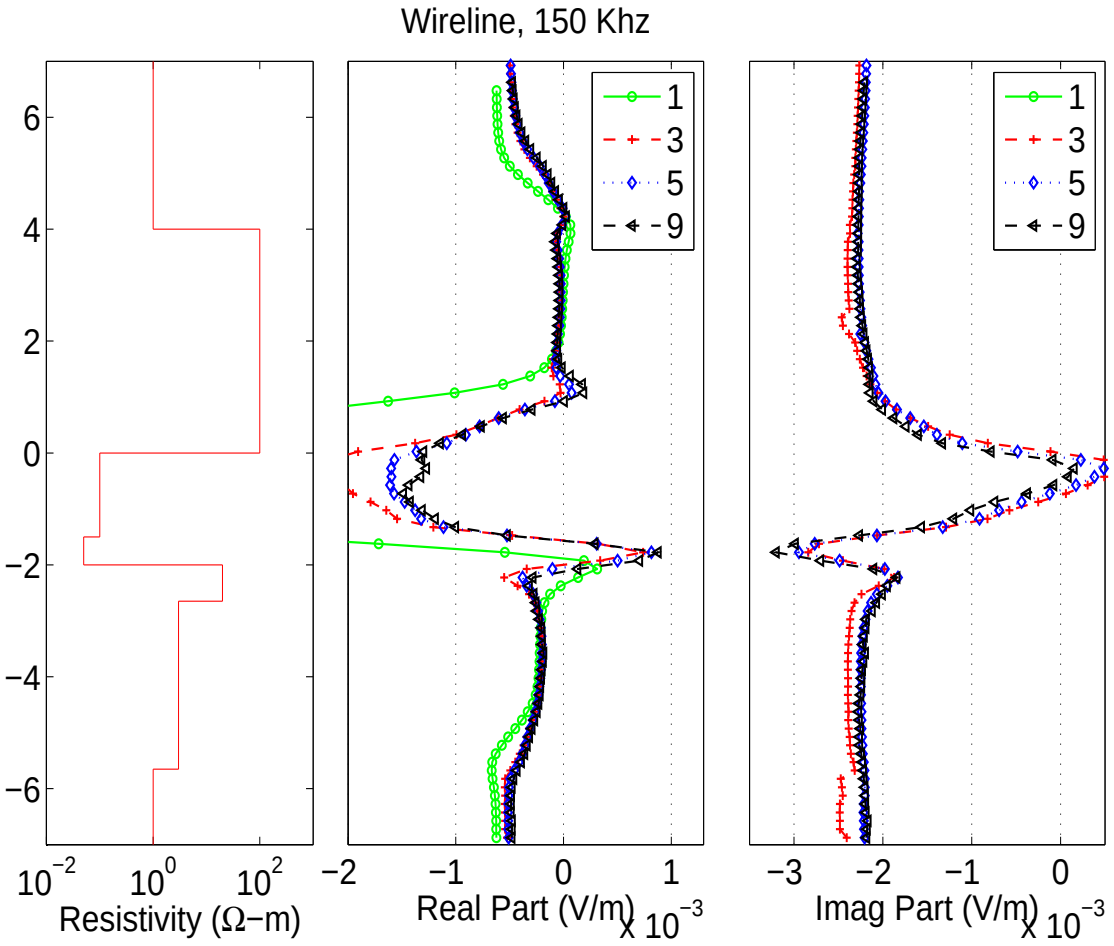

FOURIER-FINITE-ELEMENT: ILLUSTRATION

Verification

Logging Instrument in a Homogeneous Formation

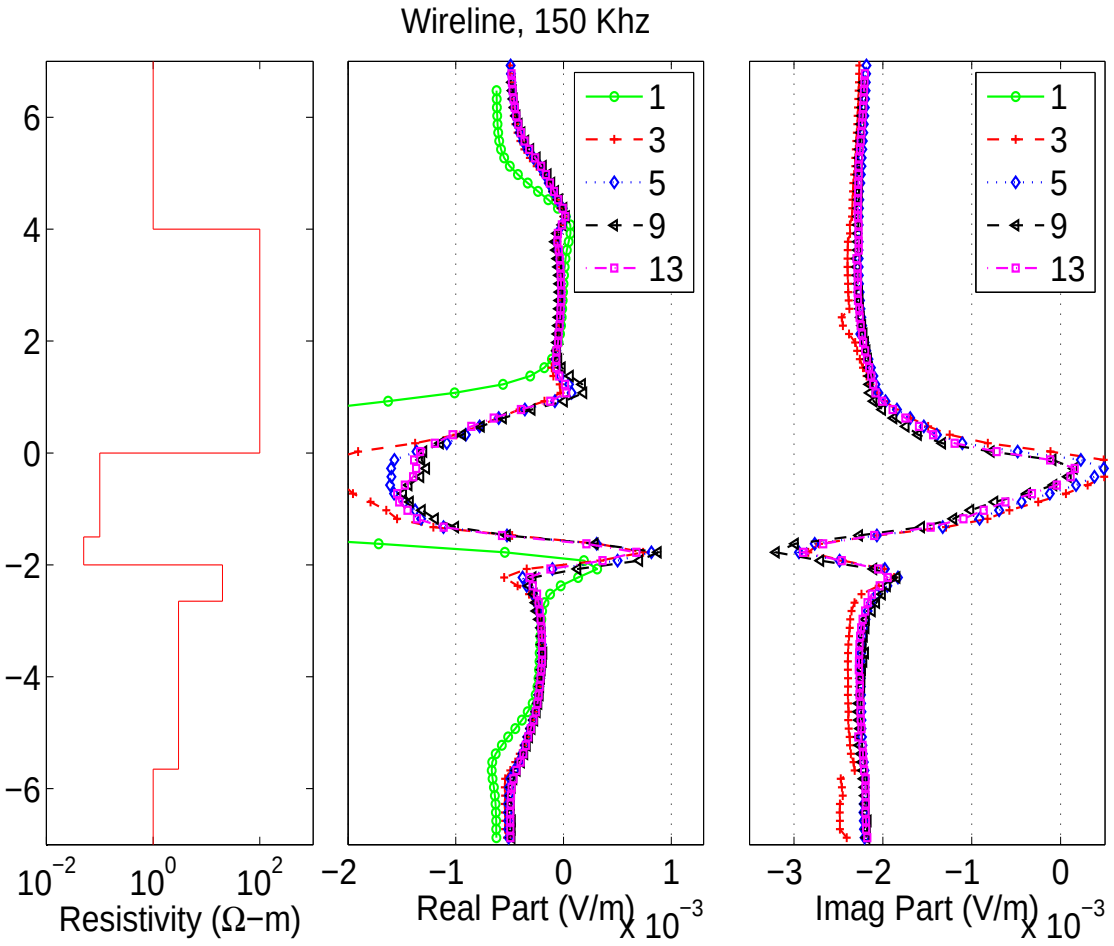

SELF-ADAPTIVE GOAL-ORIENTED HP-FEM

A Self-Adaptive Goal-Oriented hp-FEM

Optimal 2D Grid
(Through Casing Resistivity Problem)

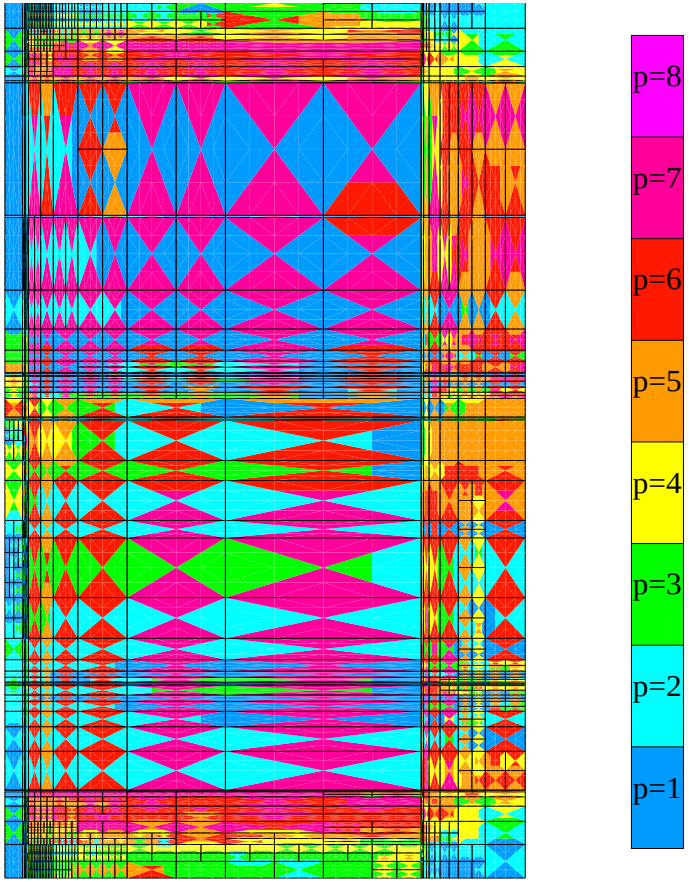

We vary locally the element size h and the polynomial order of approximation p throughout the grid.

Optimal grids are automatically generated by the computer.

The self-adaptive goal-oriented hp-FEM provides exponential convergence rates in terms of the CPU time vs. the error in a user prescribed quantity of interest.

ITERATIVE SOLVER

Description and Performance of the Iterative Solver

Block-Jacobi Preconditioner + **Krylov subspace optimization method (CG or GMRES).**

The block Jacobi preconditioner consists of a 2.5D problem defined by ignoring the couplings ocurring between the different Fourier basis functions in the original problem.

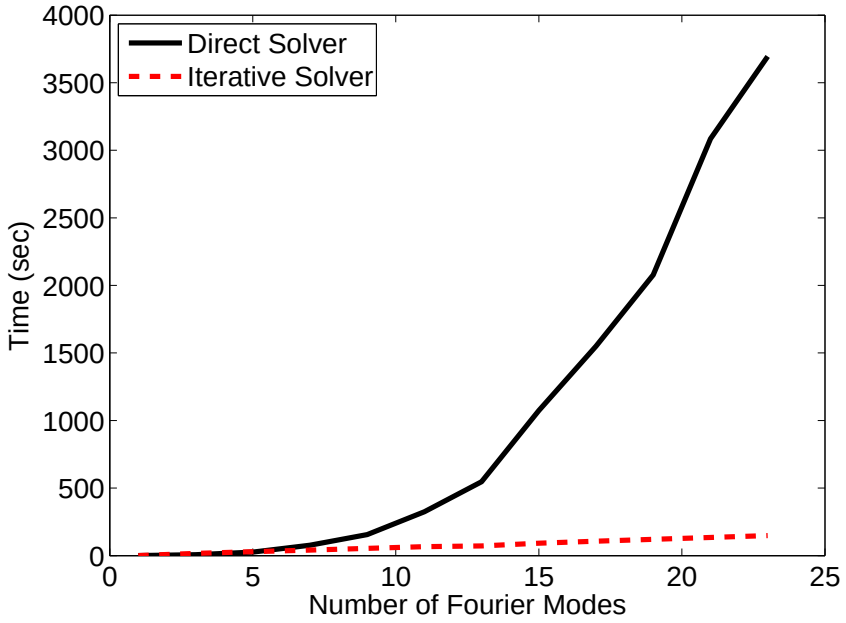

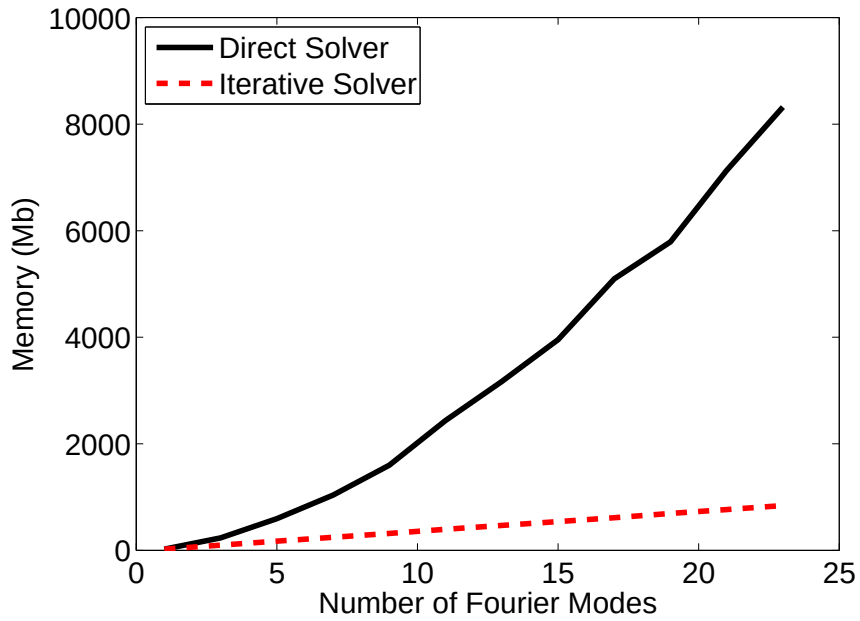

This simple iterative solver enables fast computations.

PARALLEL IMPLEMENTATION

We Use Shared Domain Decomposition

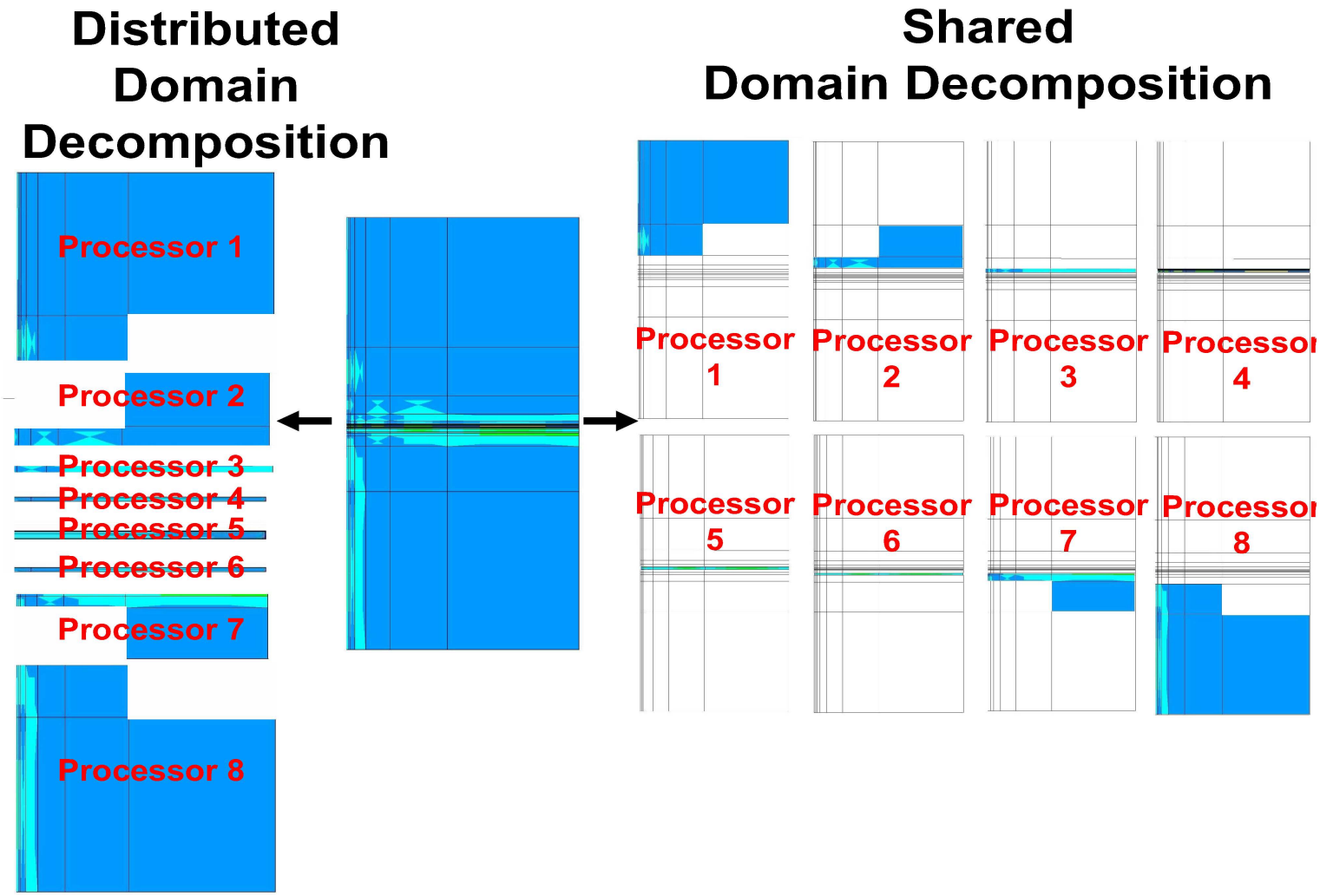

NUMERICAL RESULTS: DC RESULTS

Simulation of Through Casing Resistivity Measurements

Casing resistivity: $10^{-5} - 10^{-7} \Omega \cdot$ m

Casing thickness: 0.0127 m

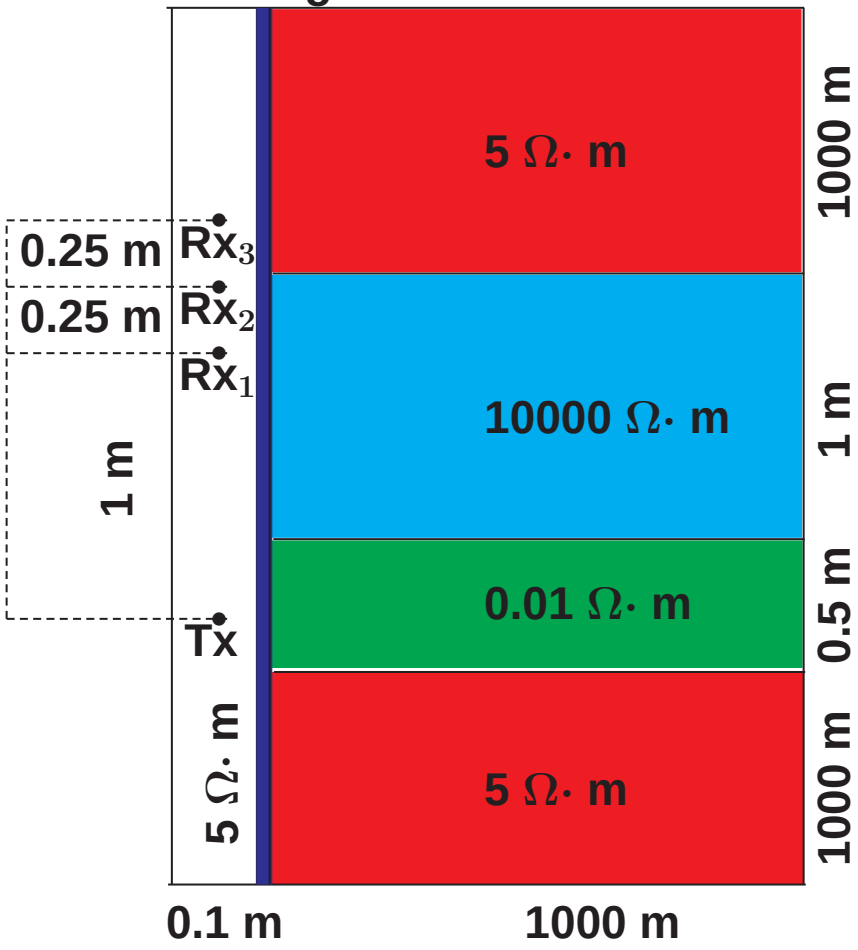

Left Figure:

- Axial-symmetric model
- One current electrode (emitter)
- Three voltage electrodes (collectors)

Objective:

- Compute second diff. of potential for various depth angles and possibly with water invasion

Method of solution:

- Fourier series expansion + change of coordinates + 2D goal-oriented hp-FEM

NUMERICAL RESULTS: DC RESULTS

Through Casing Resistivity Measurements (Casing Conductivity)

Casing Resistivity=$10^{-5}\Omega\cdot$ m **Casing Resistivity=$2.3 \times 10^{-7}\Omega\cdot$ m**

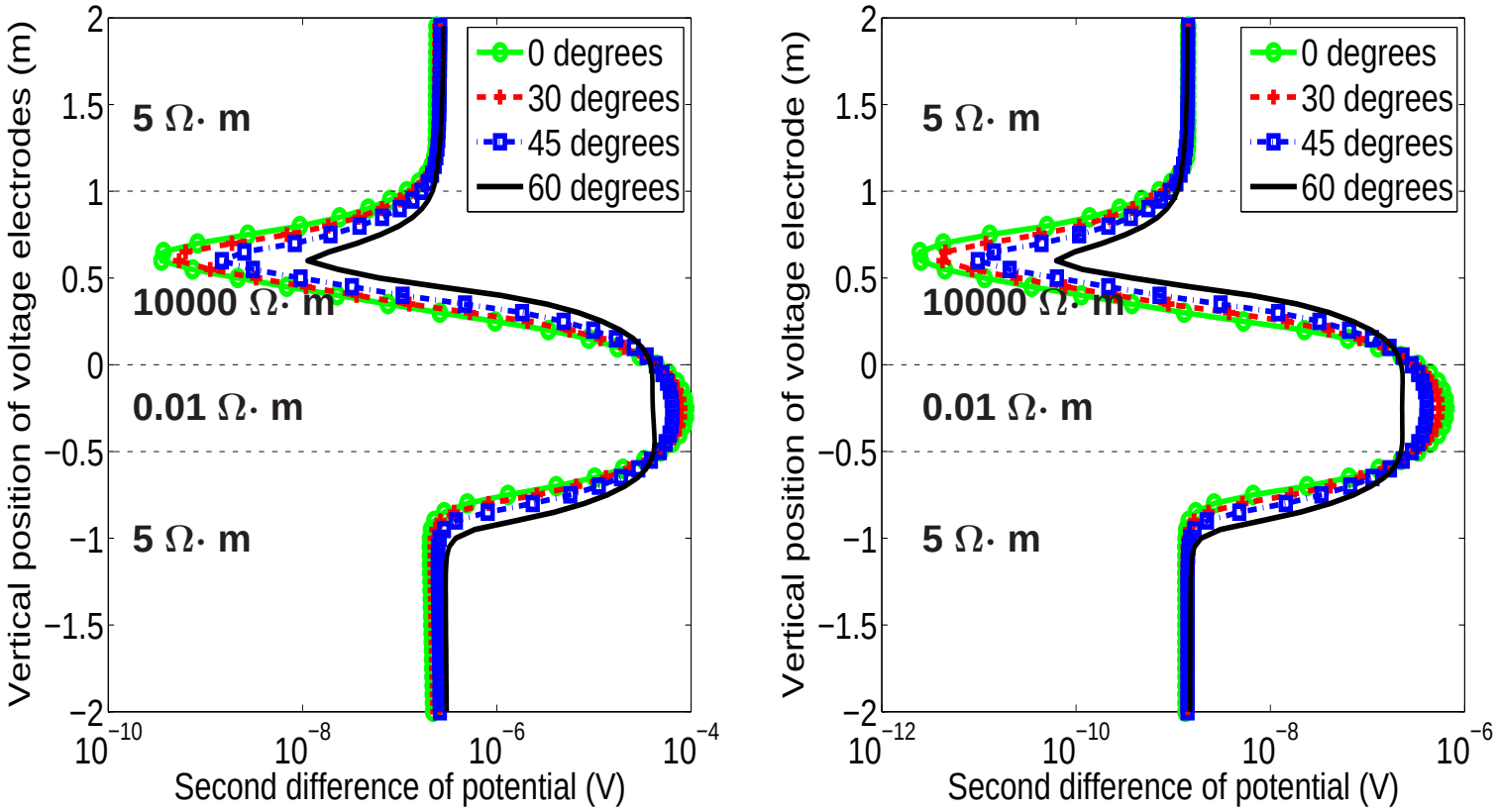

Qualitatively, results for various casing conductivities are similar even for deviated wells.

NUMERICAL RESULTS: DC RESULTS

Through Casing Resistivity Measurements (Invasion)

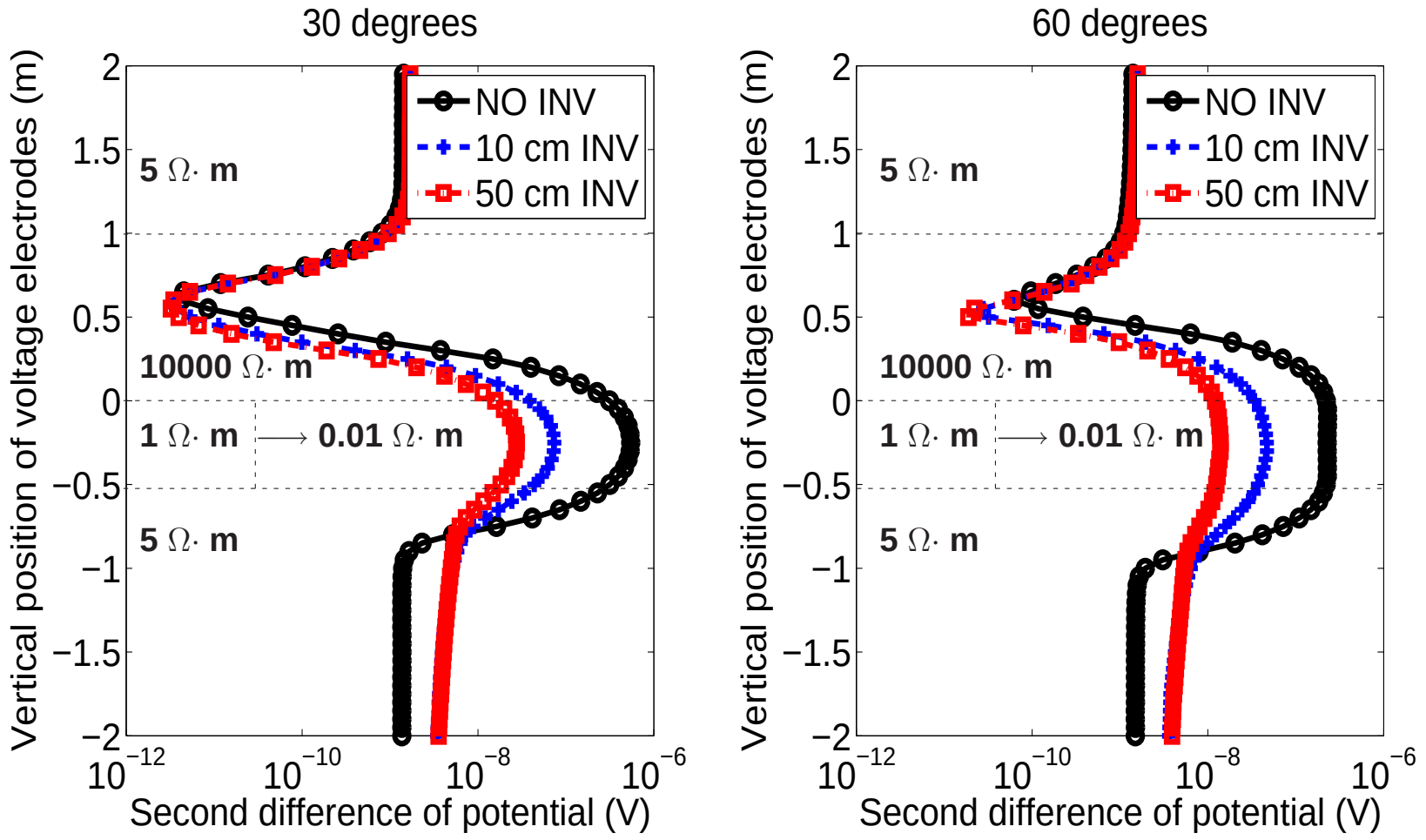

NUMERICAL RESULTS: DC RESULTS

Through Casing Resistivity Measurements (Invasion)

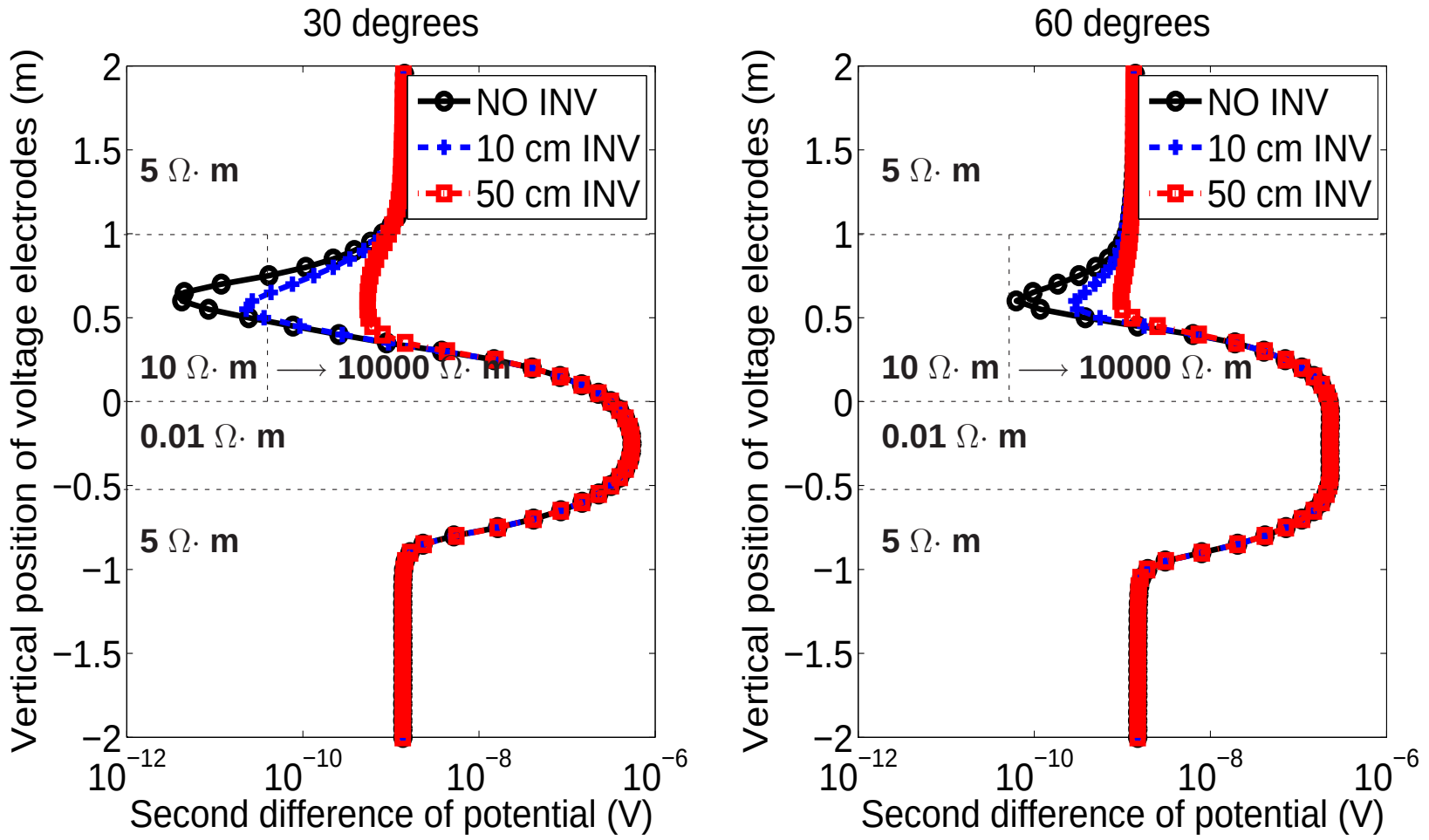

NUMERICAL RESULTS: DC LATEROLOG

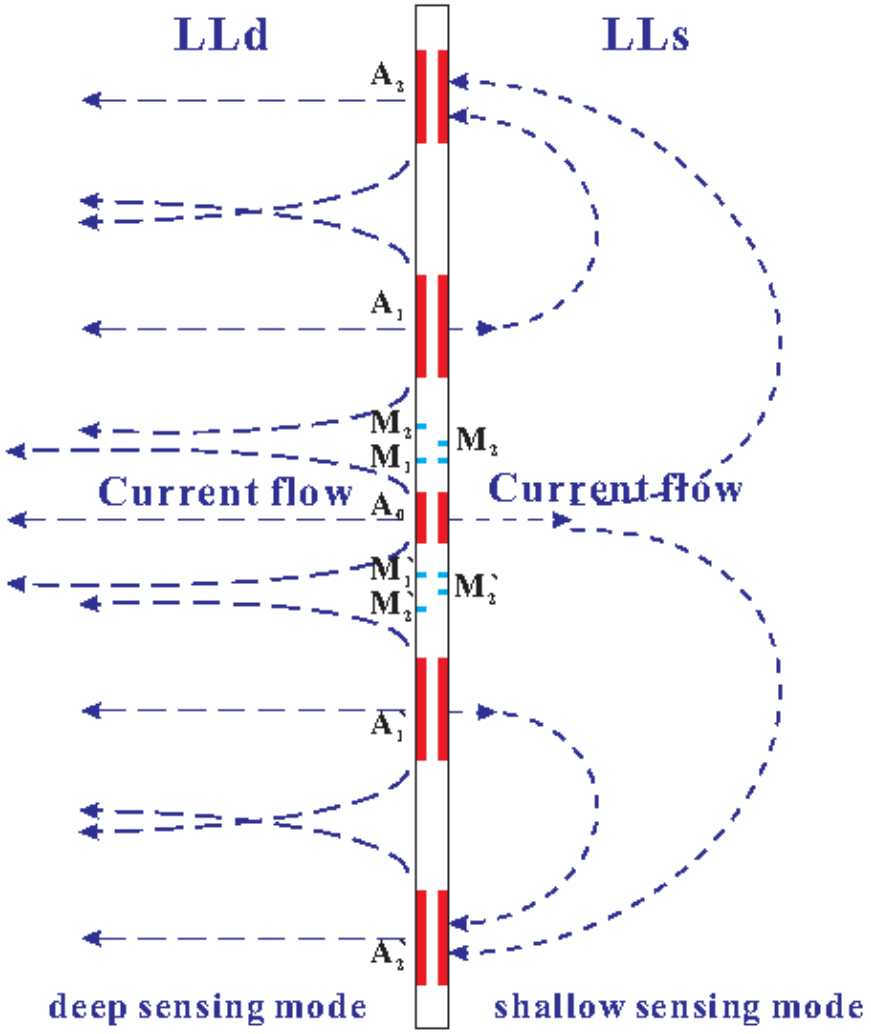

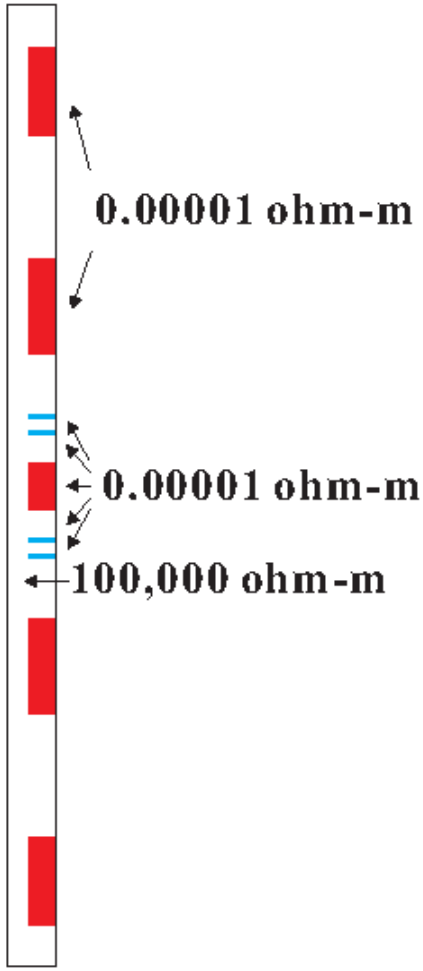

NUMERICAL RESULTS: DC LATEROLOG

Laterolog Measurements

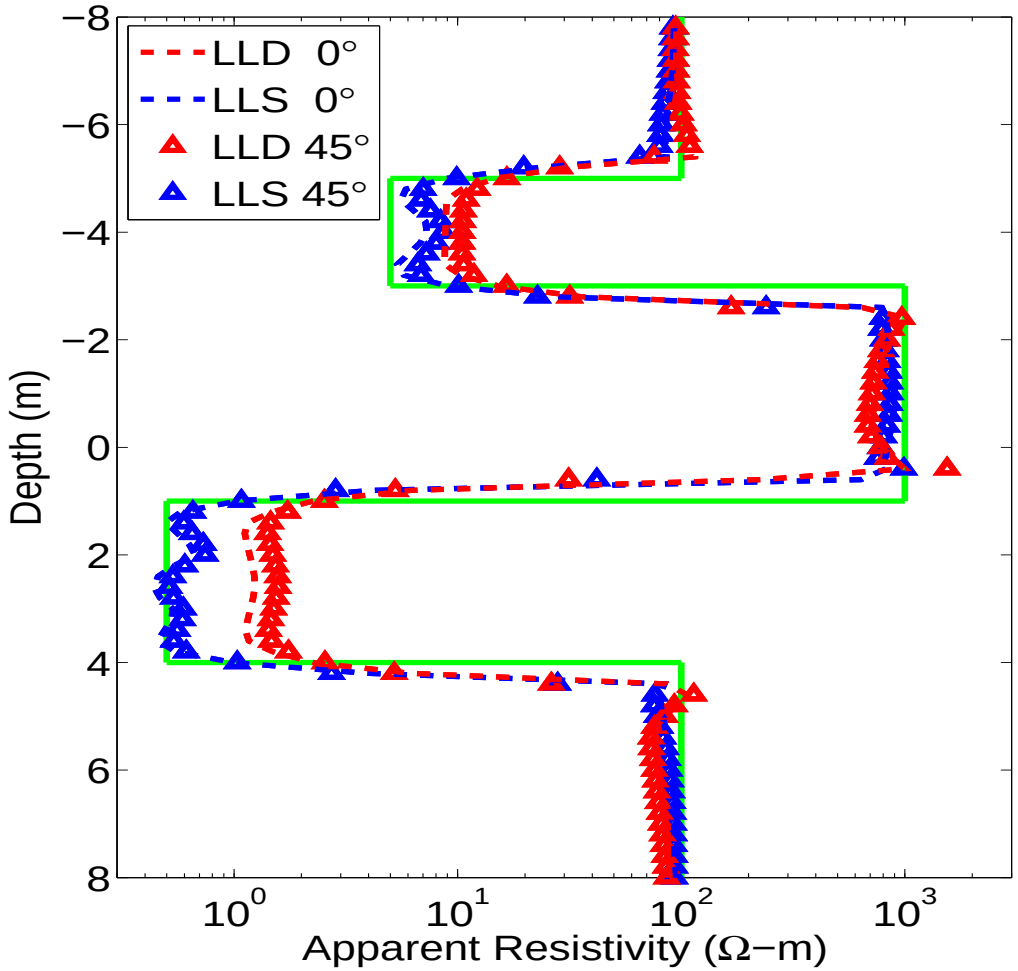

NUMERICAL RESULTS: DC LATEROLOG

ECCENTRICITY STUDY

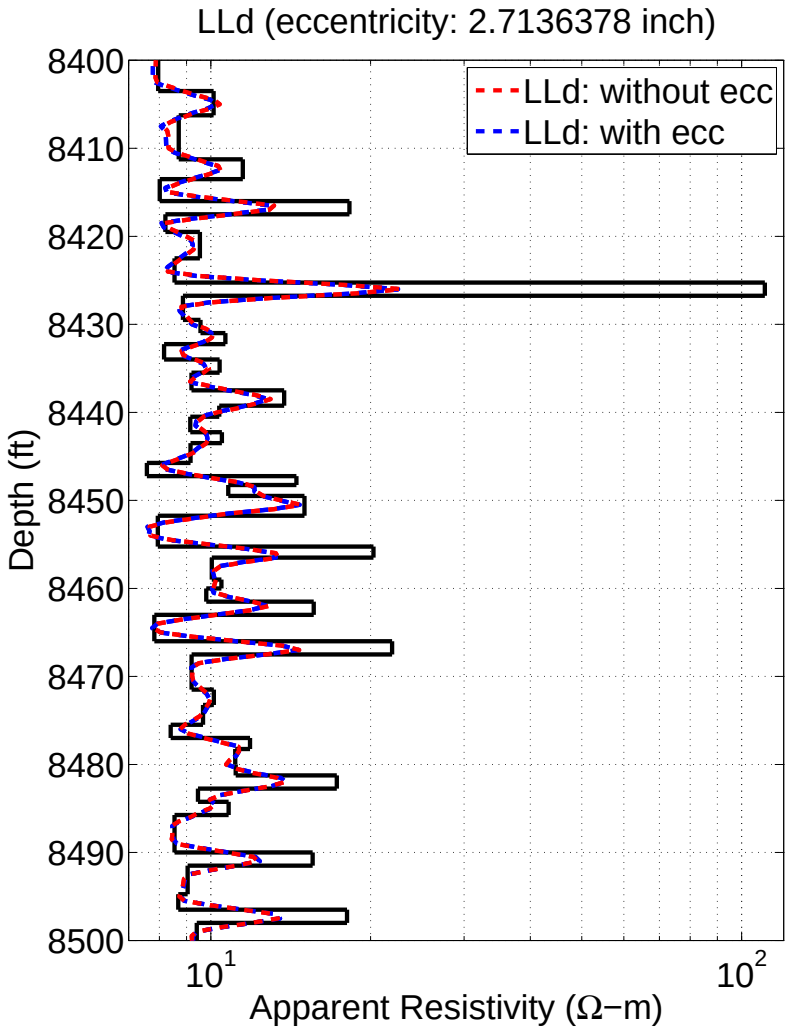

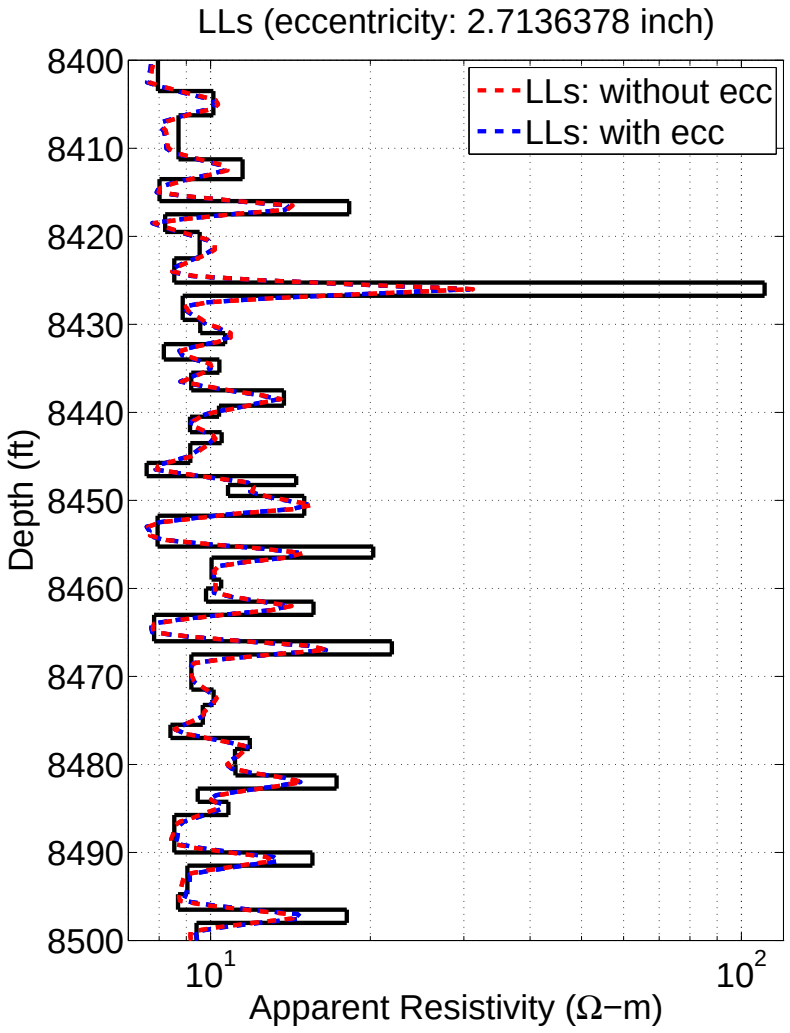

NUMERICAL RESULTS: INDUCTION

RUGOSITY STUDY: MODEL PROBLEM AT 2 MHz

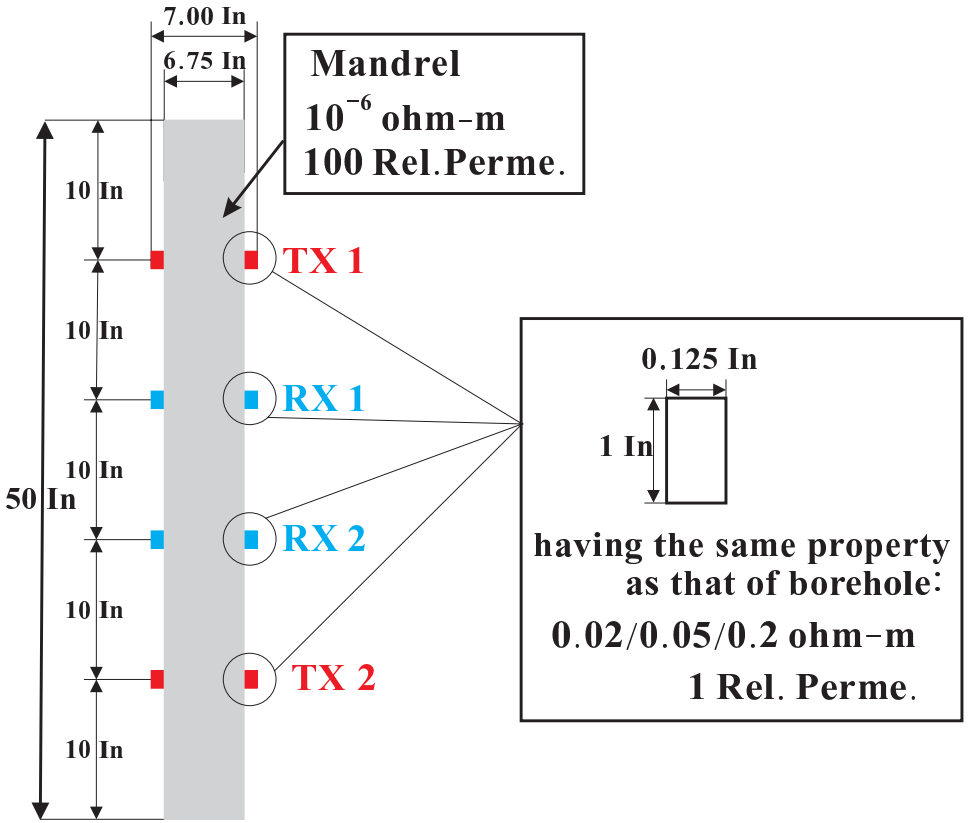

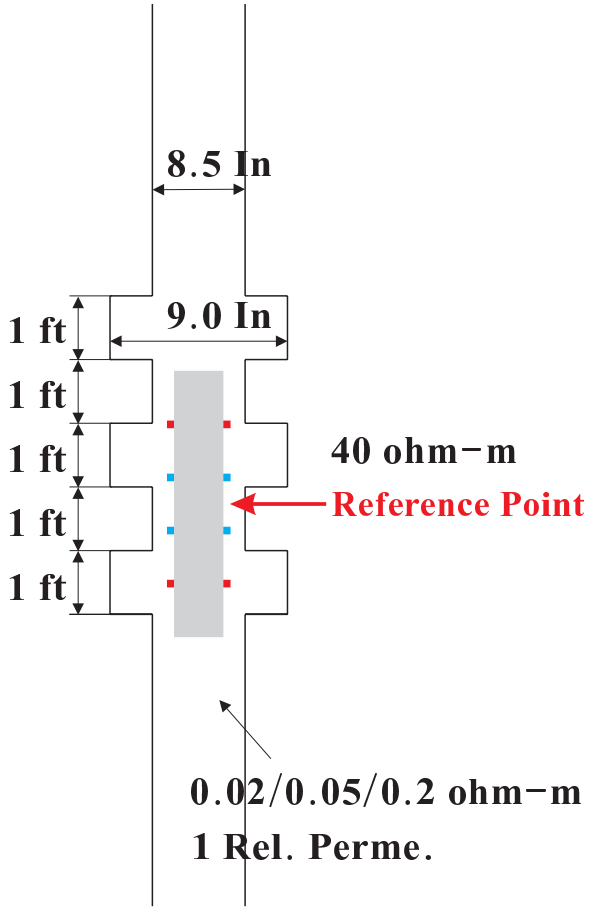

NUMERICAL RESULTS: INDUCTION

RUGOSITY STUDY (2 MHz)

TXs 1 & 2: Amp(E_ϕ)$_{RX1}$/Amp(E_ϕ)$_{RX2}$

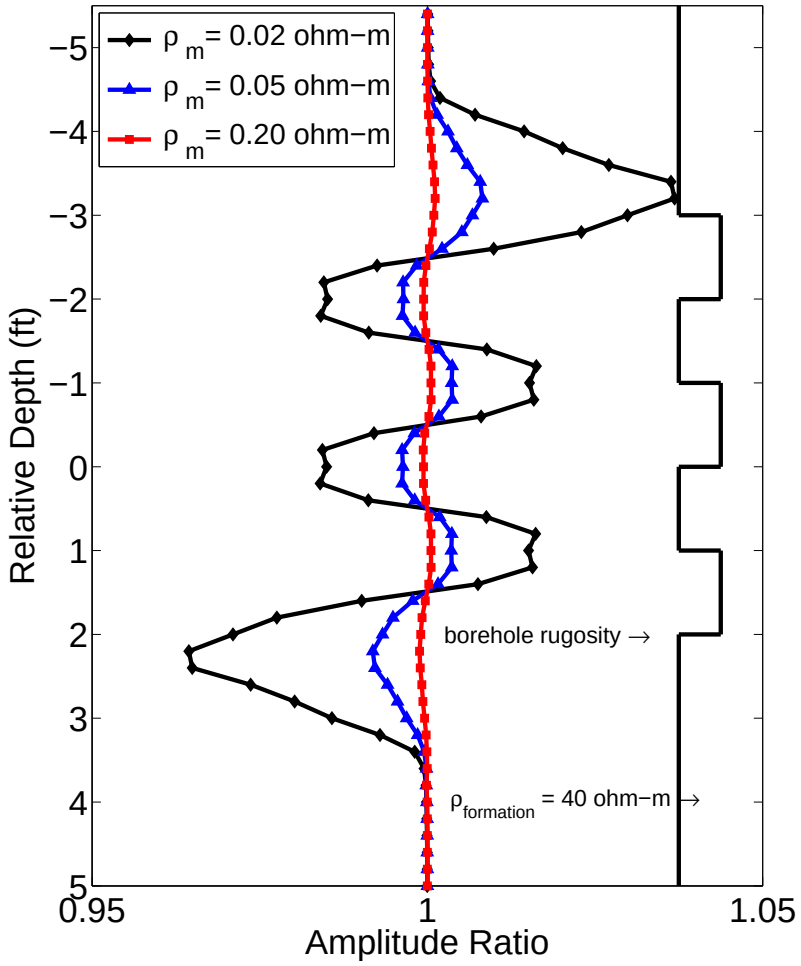

TXs 1 & 2: Phase(E_ϕ)$_{RX1}$ − Phase(E_ϕ)$_{RX2}$

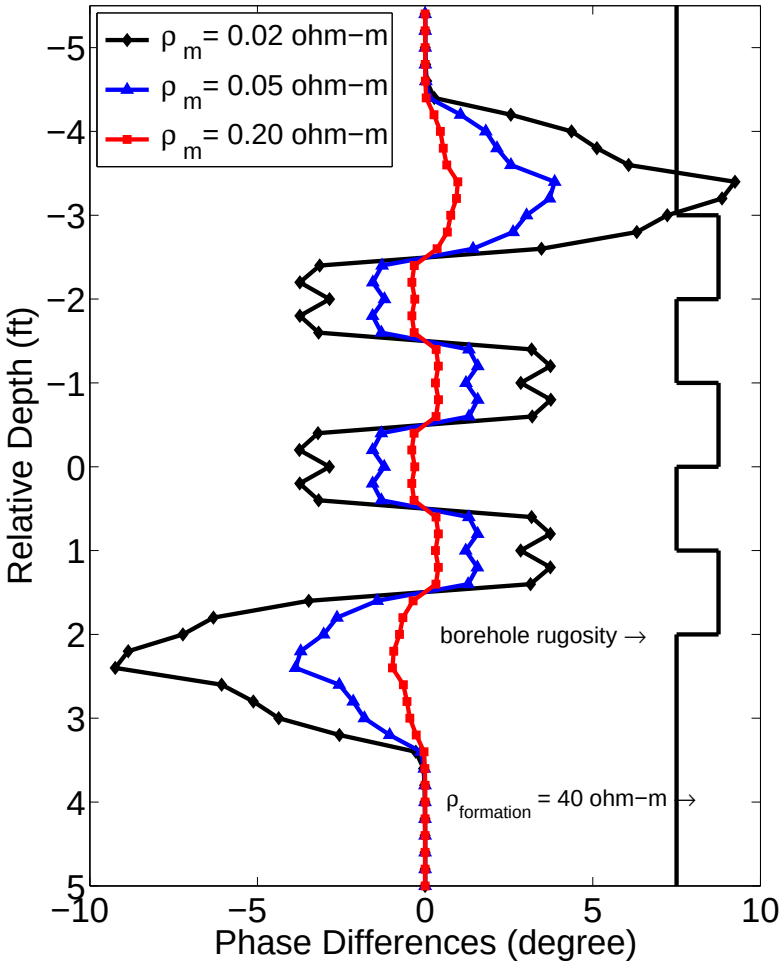

NUMERICAL RESULTS: INDUCTION

RUGOSITY STUDY (20 kHz)

TXs 1 & 2: Amp(E_ϕ)$_{RX1}$/Amp(E_ϕ)$_{RX2}$

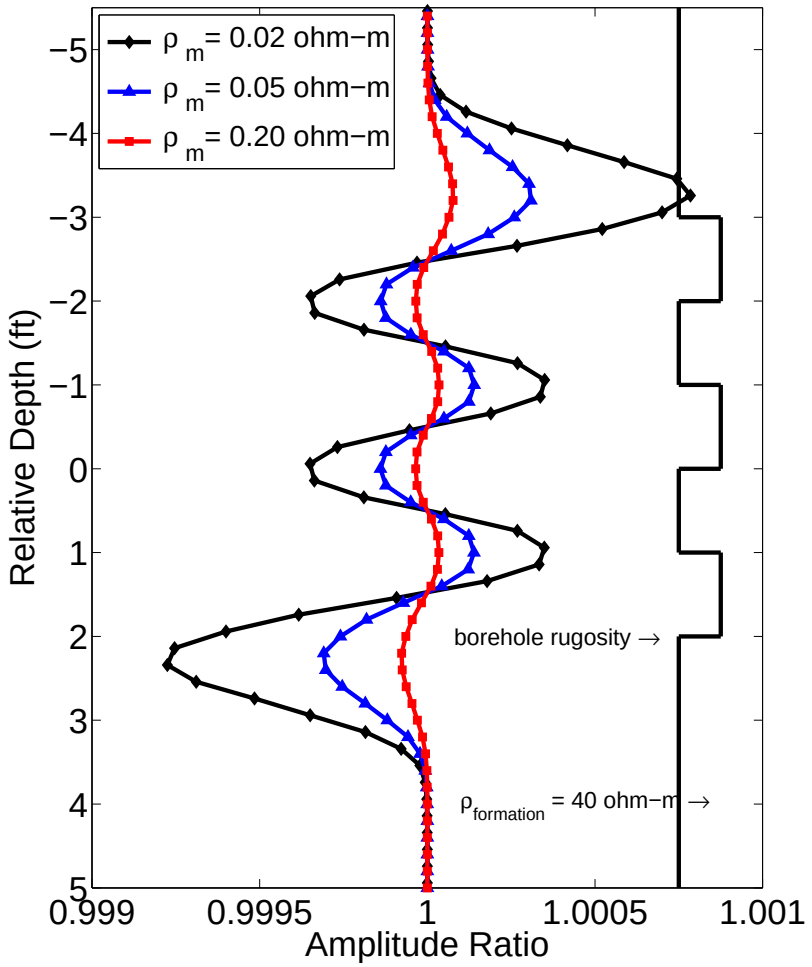

TXs 1 & 2: Phase(E_ϕ)$_{RX1}$ − Phase(E_ϕ)$_{RX2}$

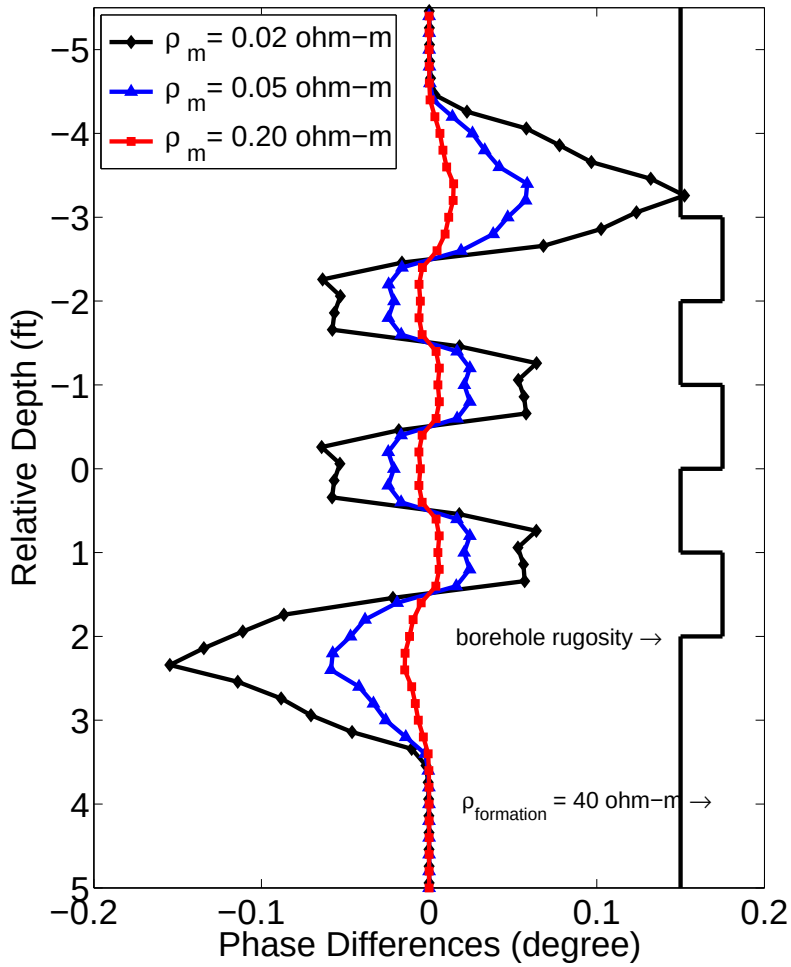

NUMERICAL RESULTS: INDUCTION

Model Problem

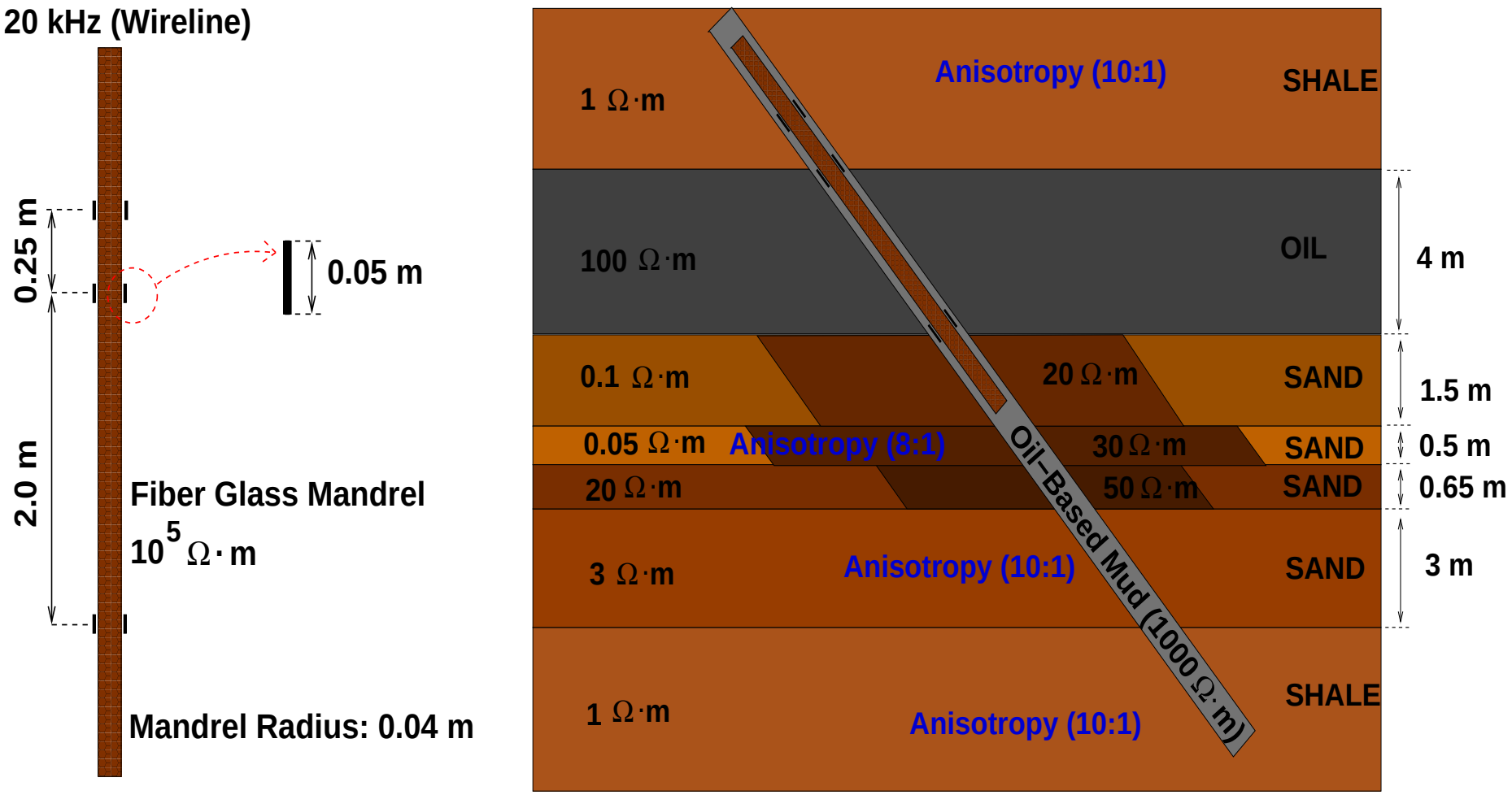

NUMERICAL RESULTS: INDUCTION

Verification

Logging Instrument in a Homogeneous Formation

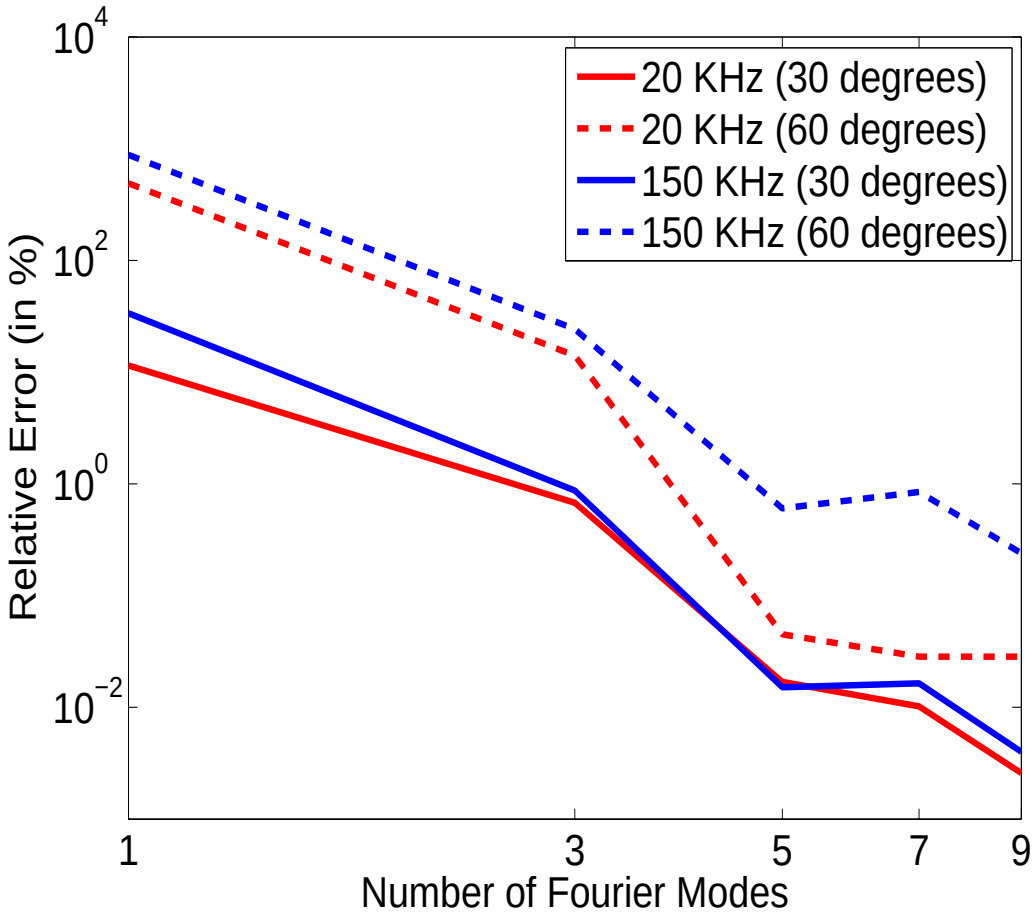

NUMERICAL RESULTS: INDUCTION

Dip Angle

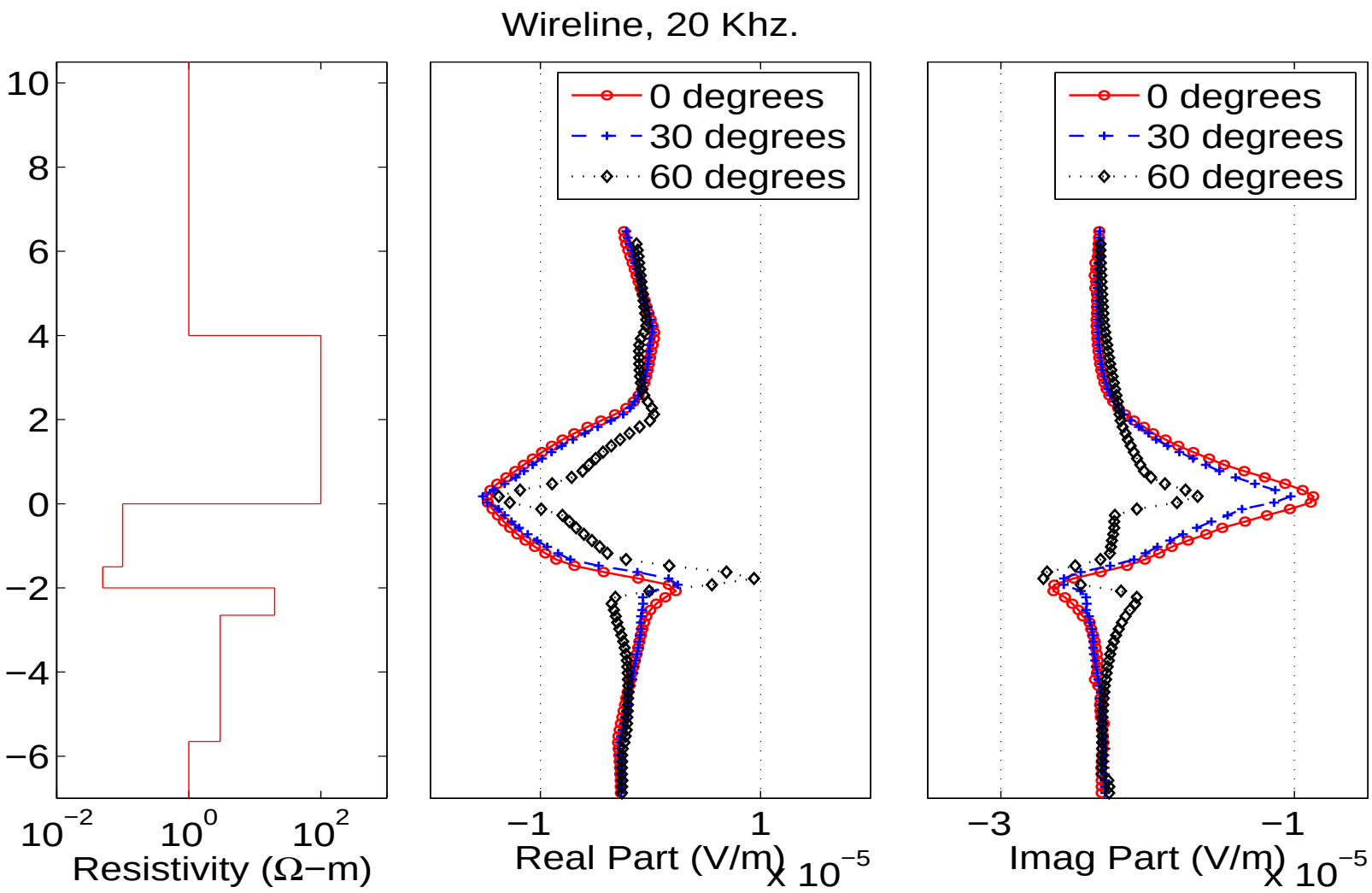

NUMERICAL RESULTS: INDUCTION

Dip Angle + Invasion

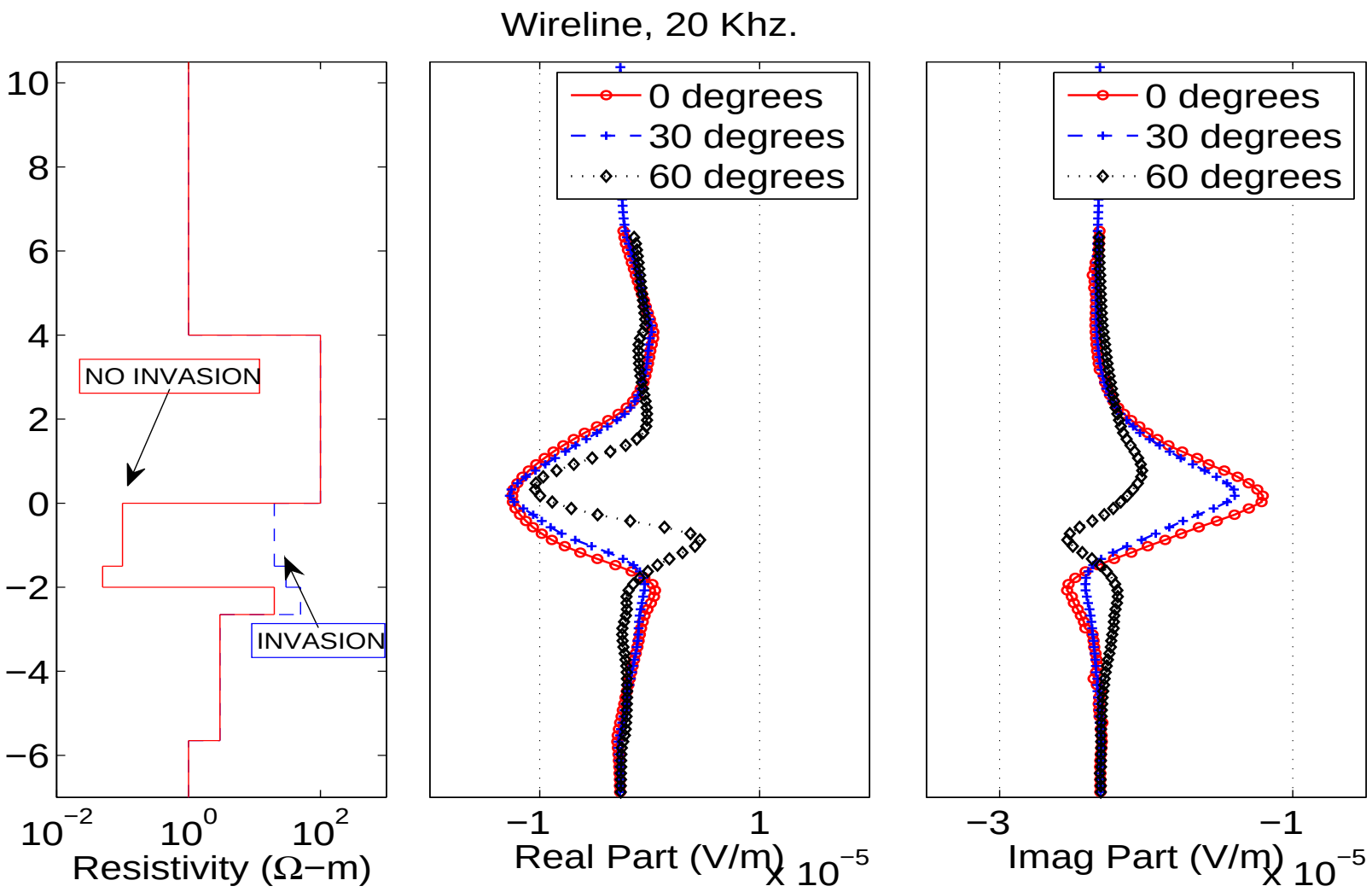

NUMERICAL RESULTS: INDUCTION

Dip Angle + Anisotropy

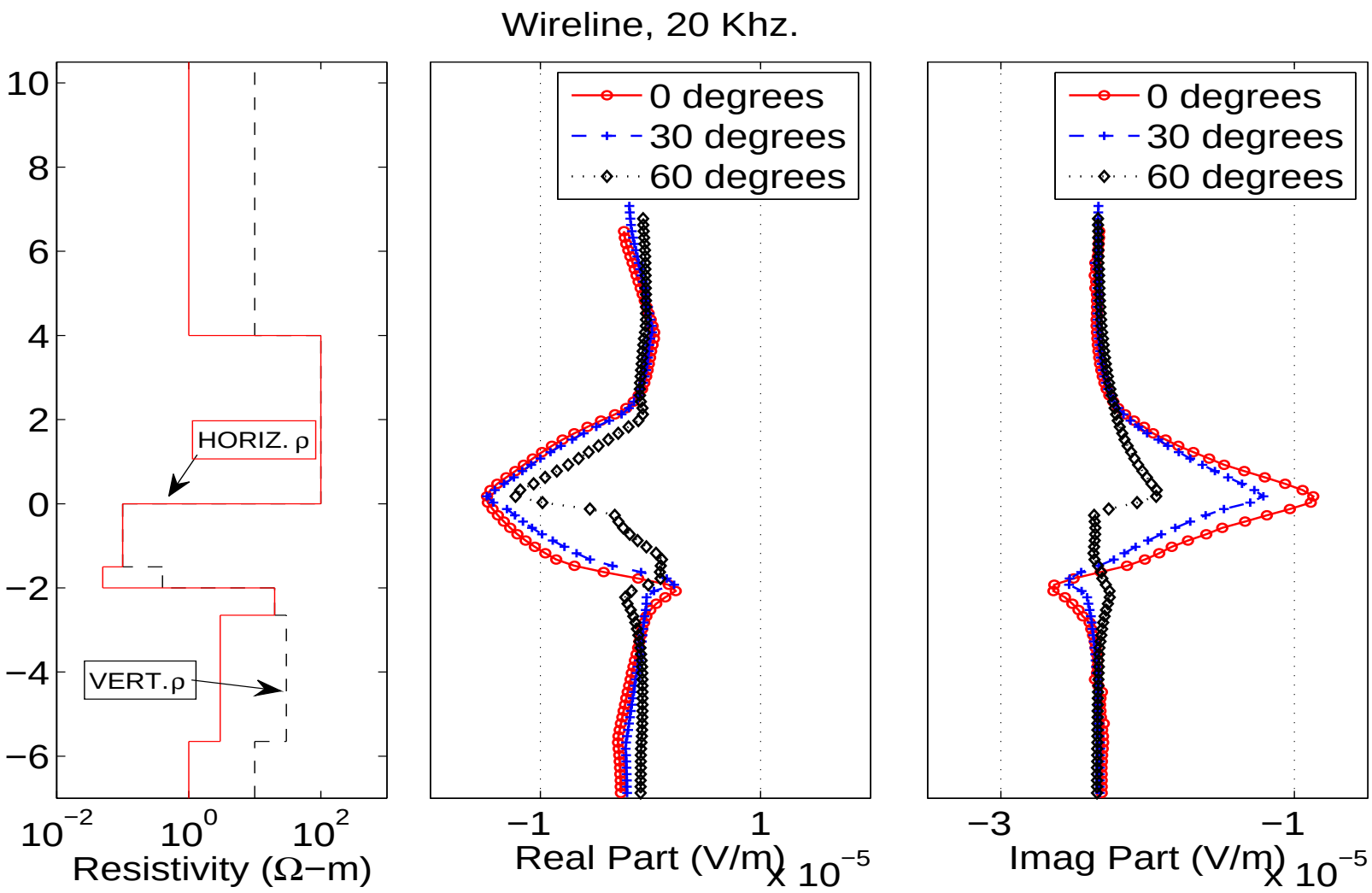

NUMERICAL RESULTS: INDUCTION

Dip Angle + Invasion + Anisotropy

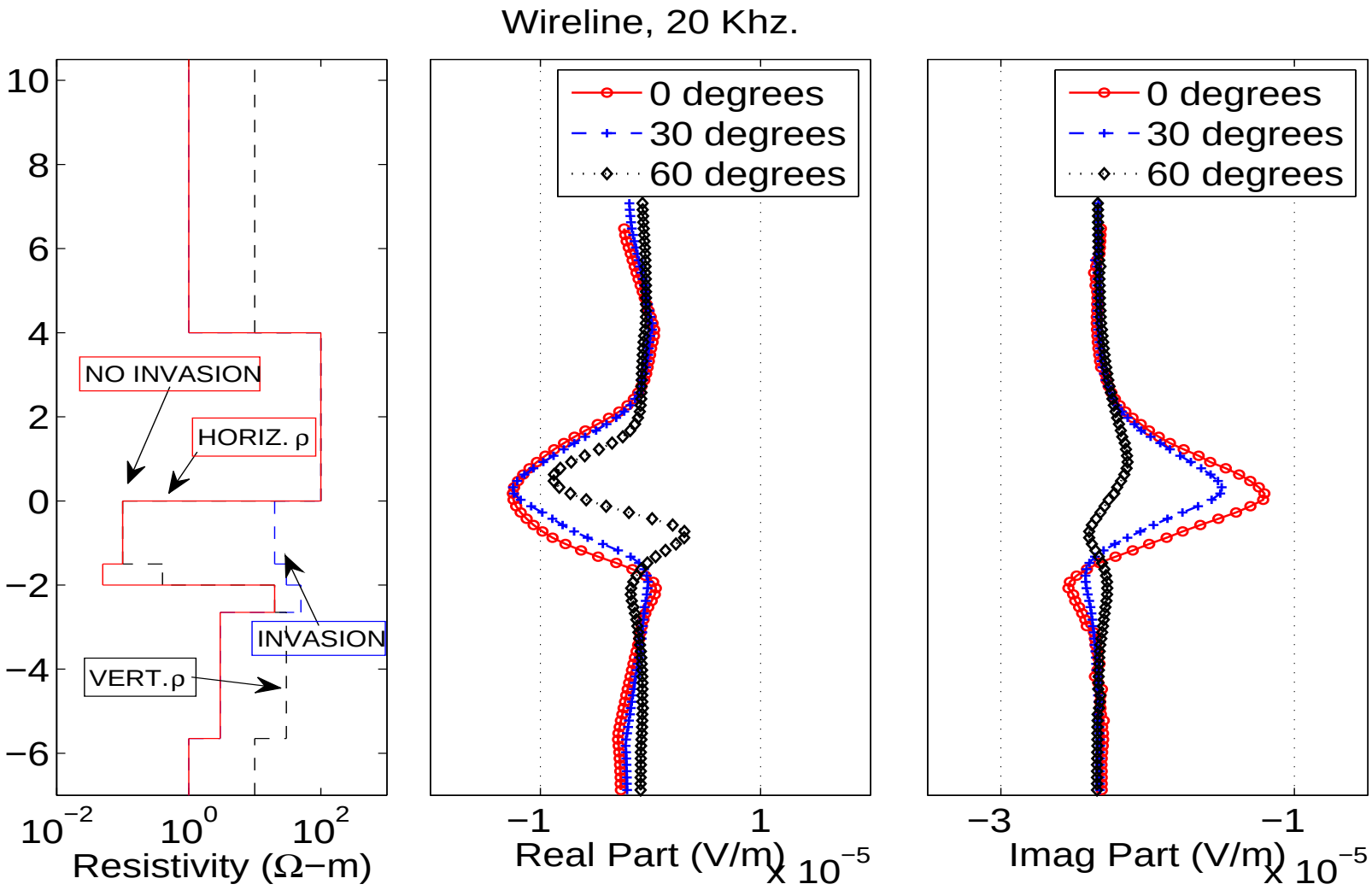

NUMERICAL RESULTS: INDUCTION

60-Degree Deviated Well

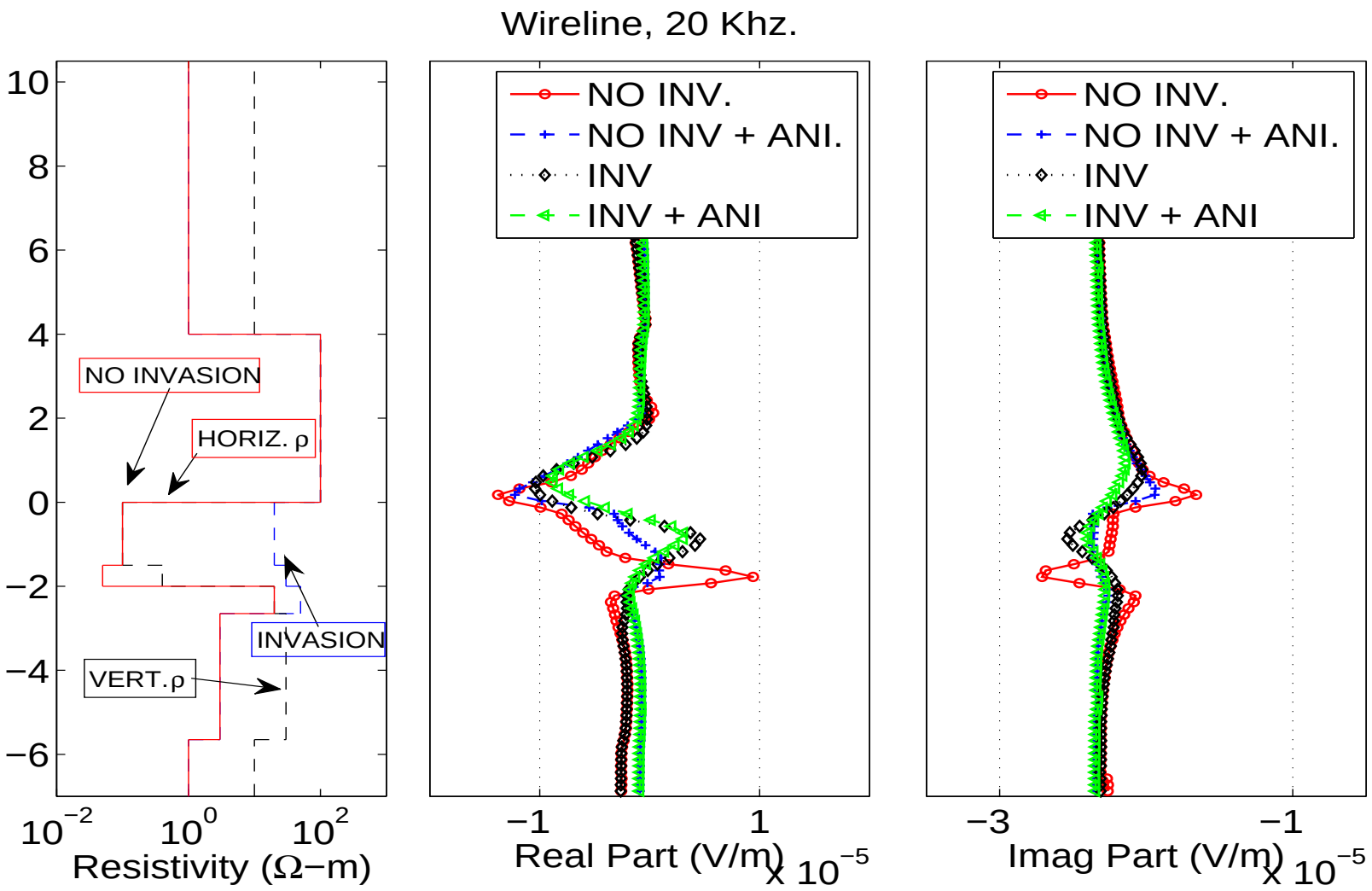

NUMERICAL RESULTS: INDUCTION

Model Problem and Verification

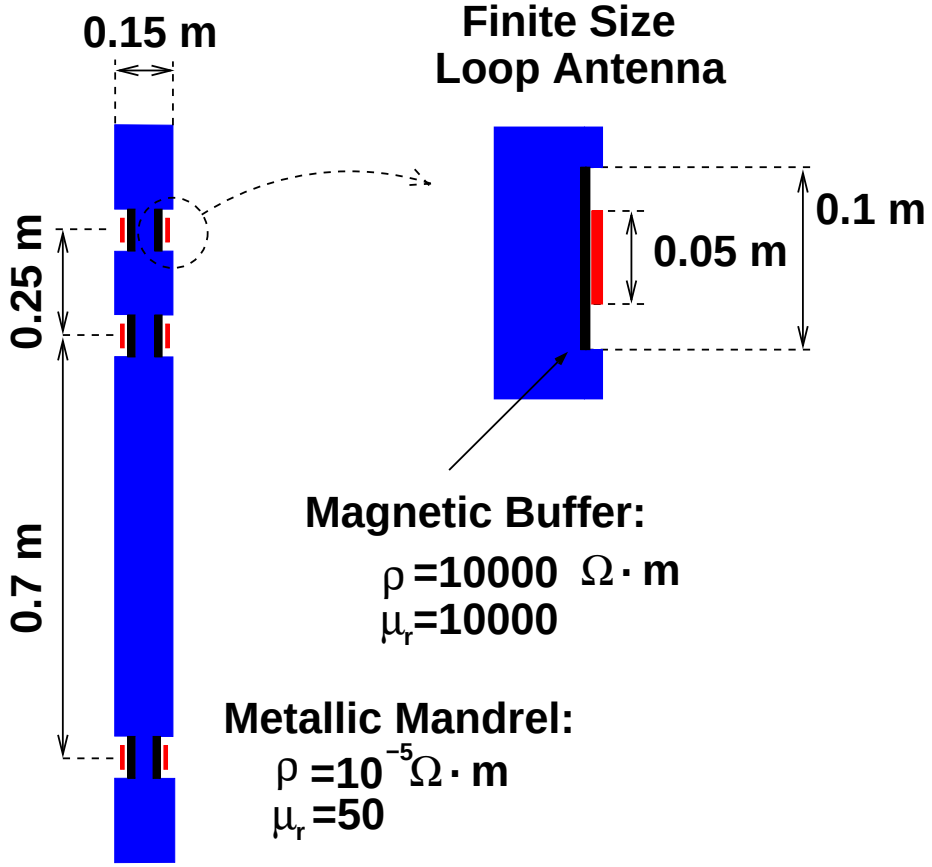

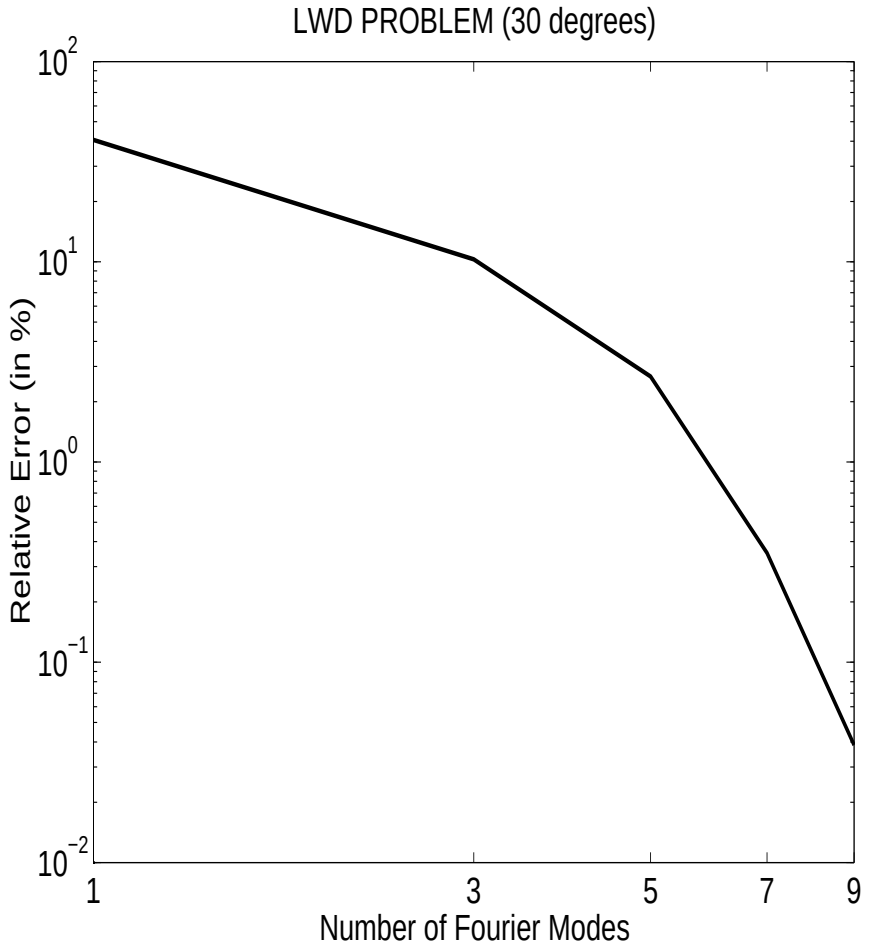

NUMERICAL RESULTS: INDUCTION

Dip Angle

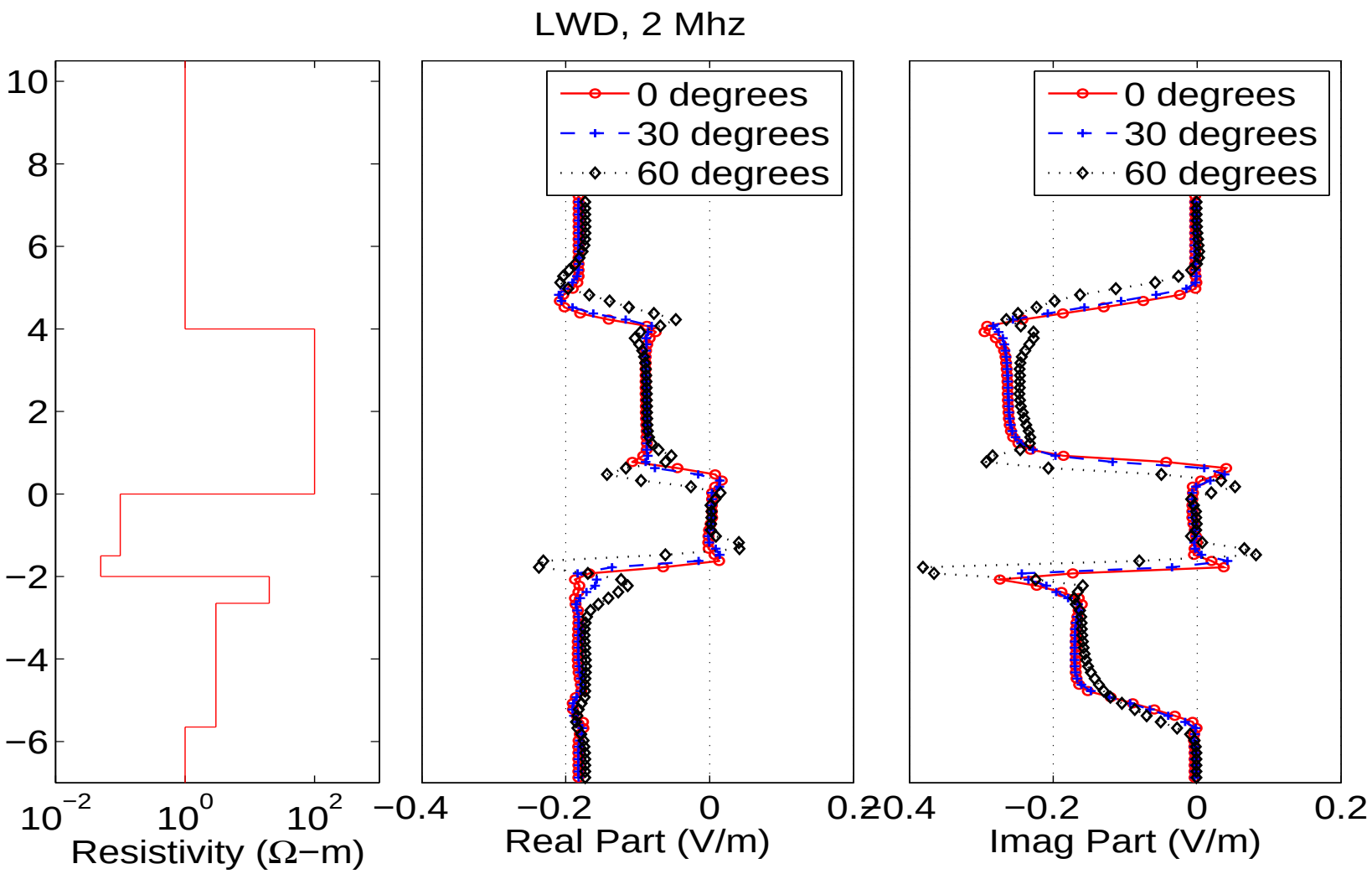

NUMERICAL RESULTS: INDUCTION

Dip Angle + Invasion

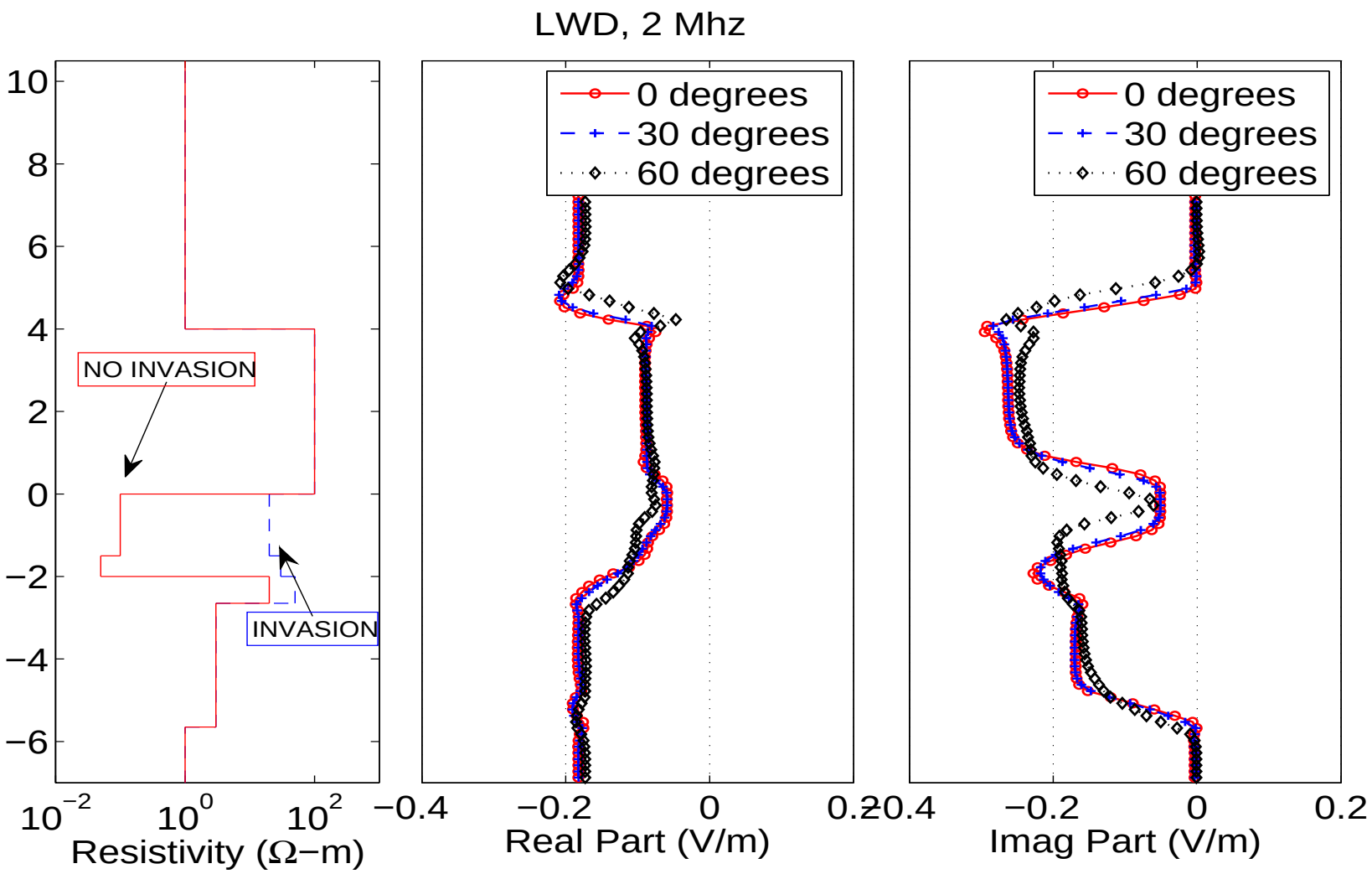

NUMERICAL RESULTS: INDUCTION

Dip Angle + Anisotropy

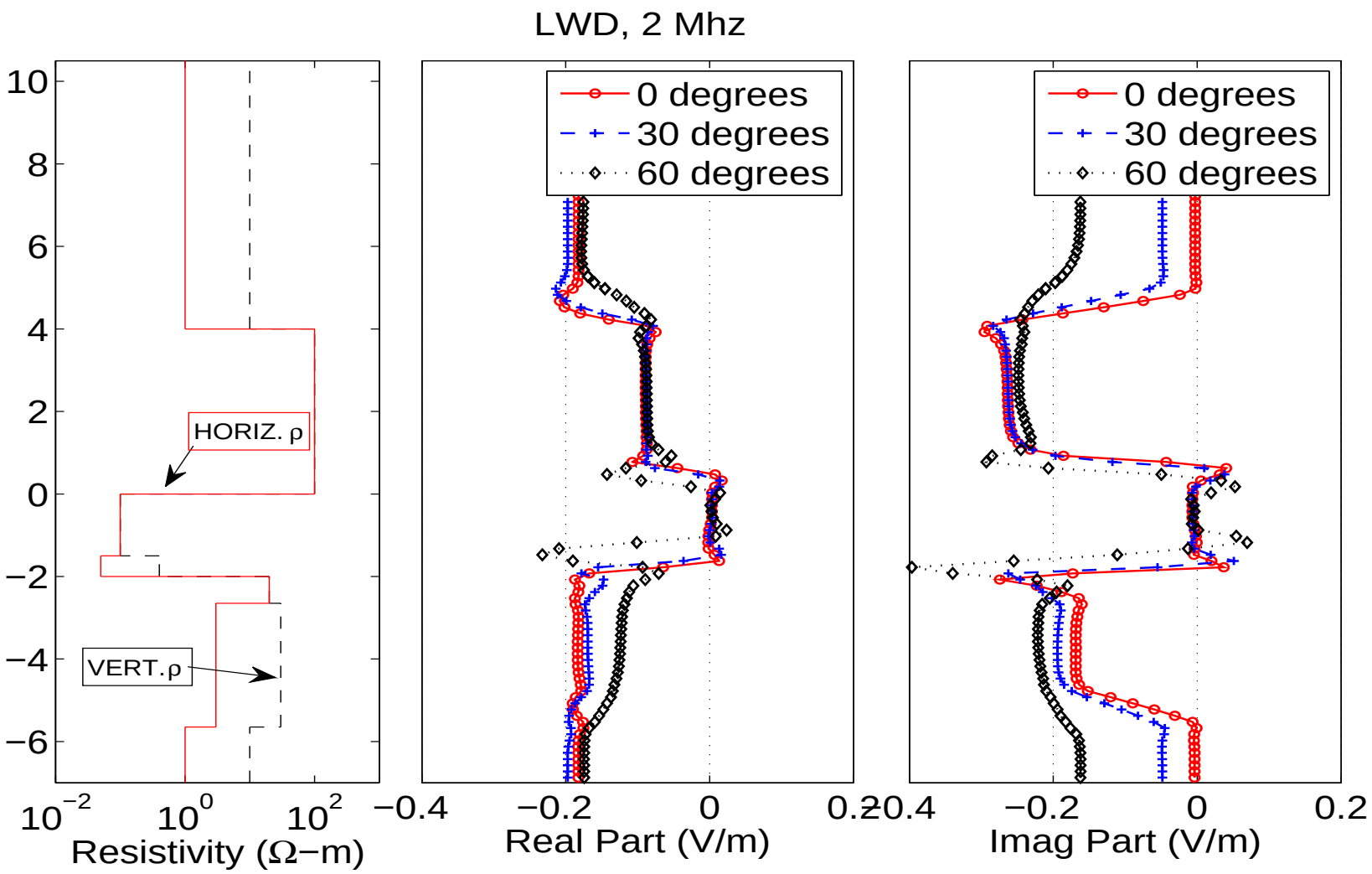

NUMERICAL RESULTS: INDUCTION

Dip Angle + Invasion + Anisotropy

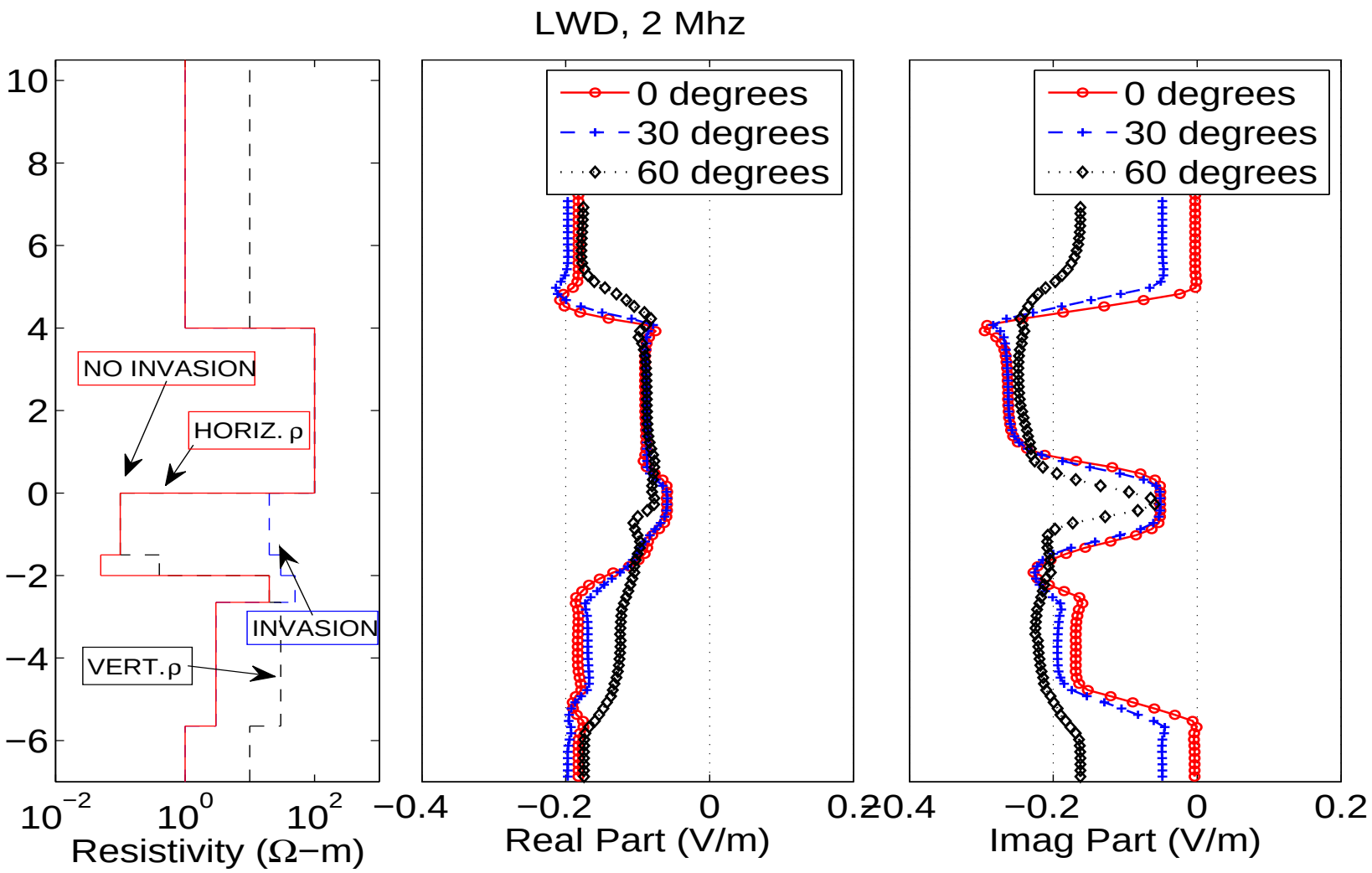

NUMERICAL RESULTS: INDUCTION

60-Degree Deviated Well

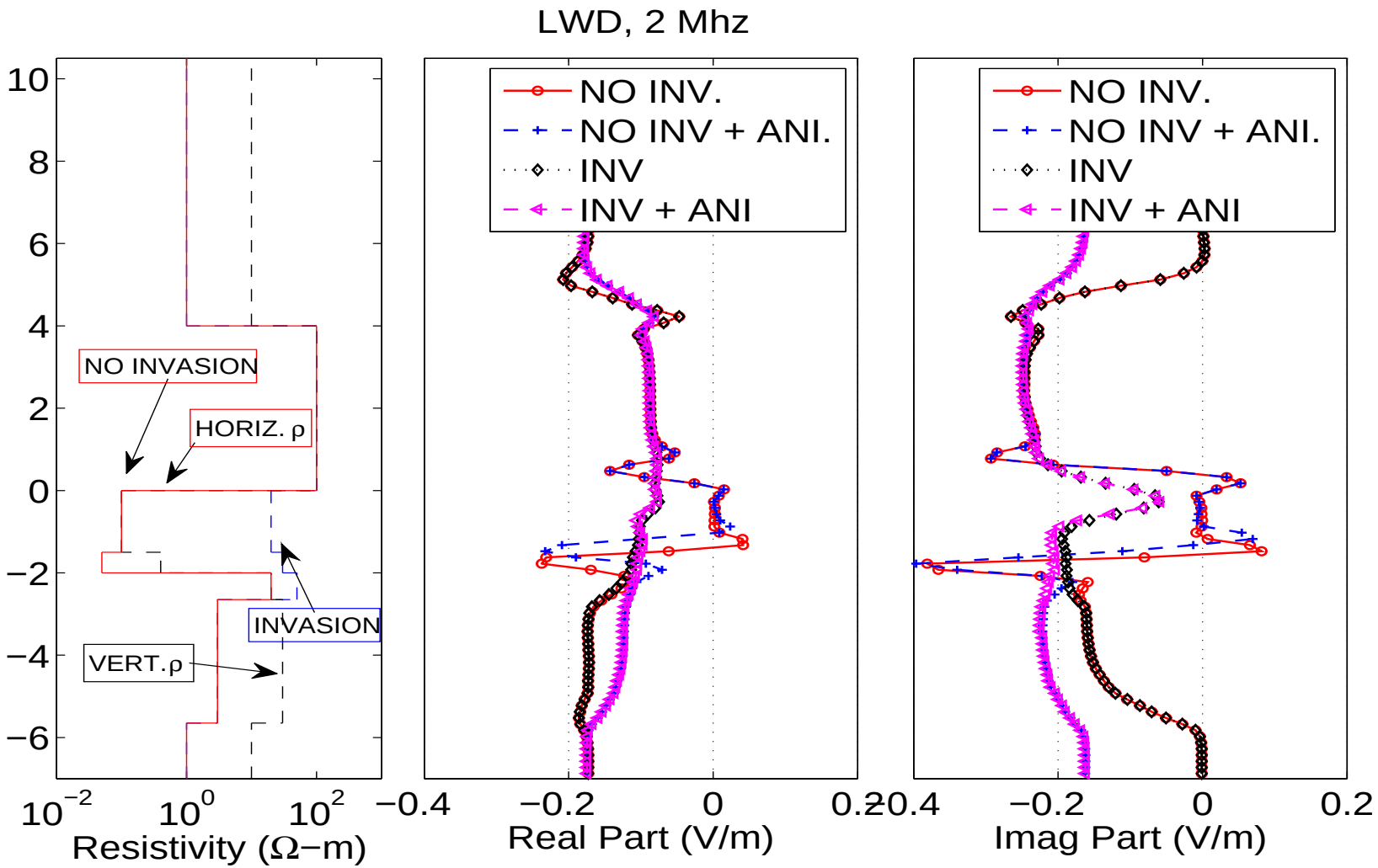

TRIAXIAL INDUCTION

2.5D Problem (Triaxial Induction). Source: Horizontal Magnetic Dipole

Mode 0 (H_ϕ)

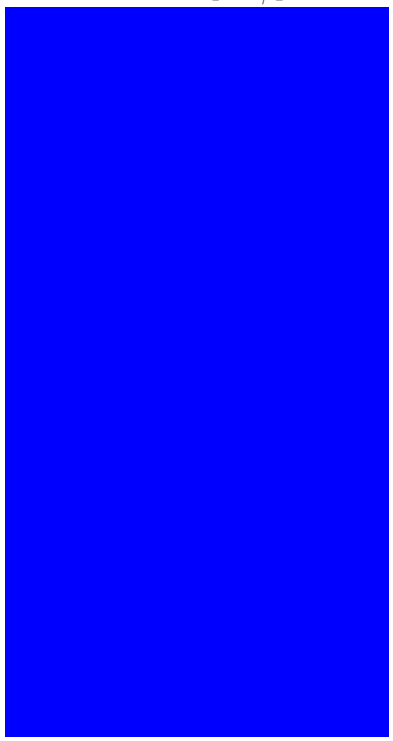

Mode 1 (H_ϕ)

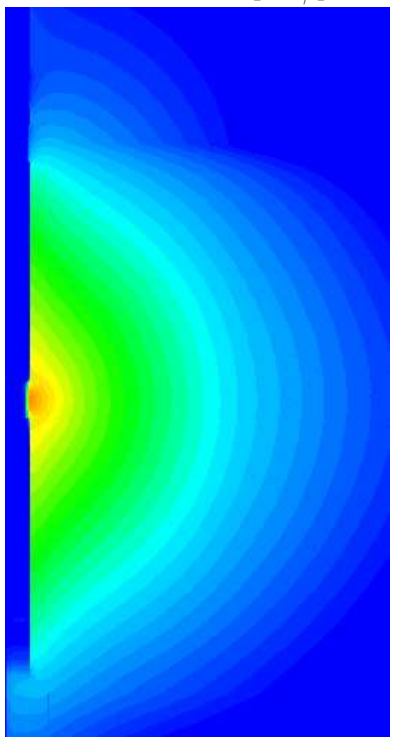

Mode 2 (H_ϕ)

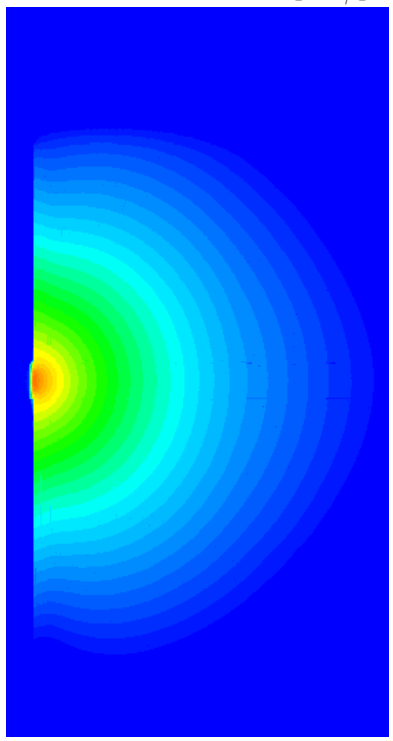

EXAMPLE OF 2.5D TRIAXIAL INDUCTION LWD PROBLEM

TRIAXIAL INDUCTION

2.5D Problem (Triaxial Induction). Source: Horizontal Magnetic Dipole

Mode 0 (H_ρ)

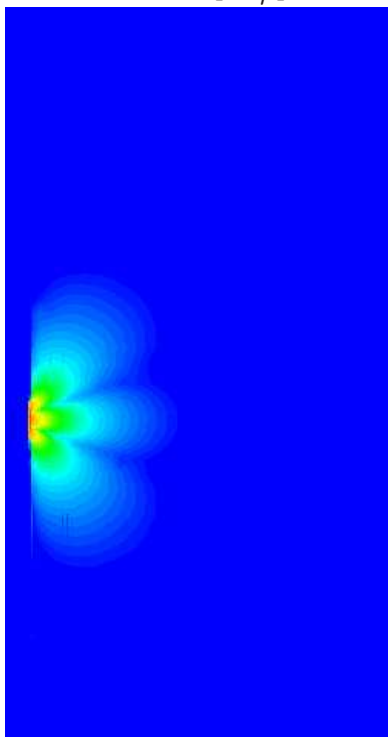

Mode 1 (H_ρ)

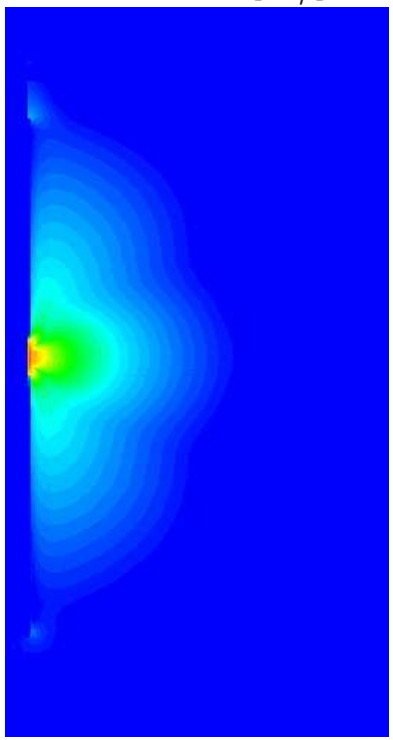

Mode 2 (H_ρ)

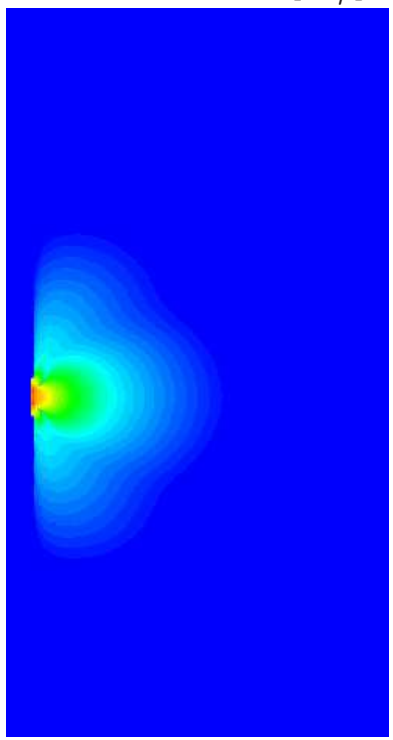

EXAMPLE OF 2.5D TRIAXIAL INDUCTION LWD PROBLEM

TRIAXIAL INDUCTION

2.5D Problem (Triaxial Induction). Source: Horizontal Magnetic Dipole

Mode 0 (H_z)

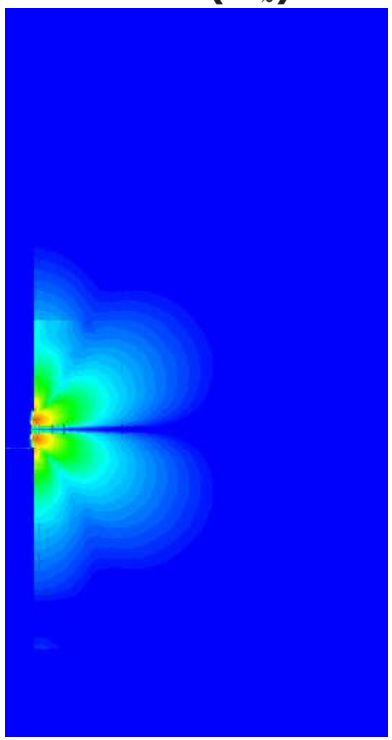

Mode 1 (H_z)

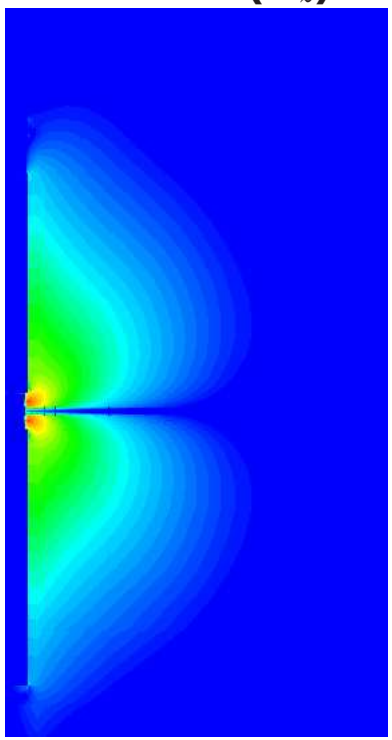

Mode 2 (H_z)

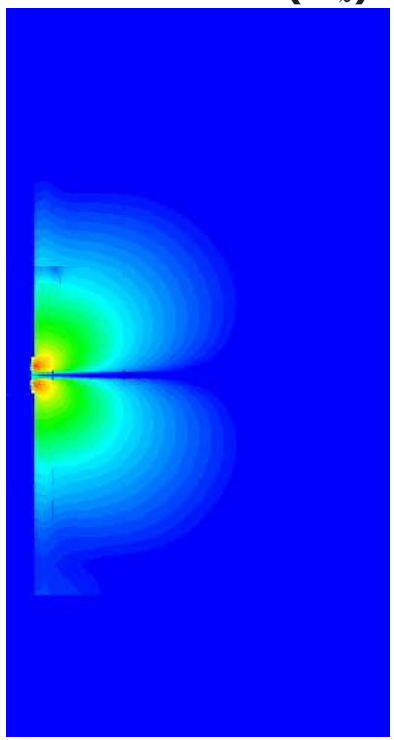

EXAMPLE OF 2.5D TRIAXIAL INDUCTION LWD PROBLEM

TRIAXIAL INDUCTION

2.5D Problem (Triaxial Induction). Source: Horizontal Magnetic Dipole

Mode 0 (H_ϕ)

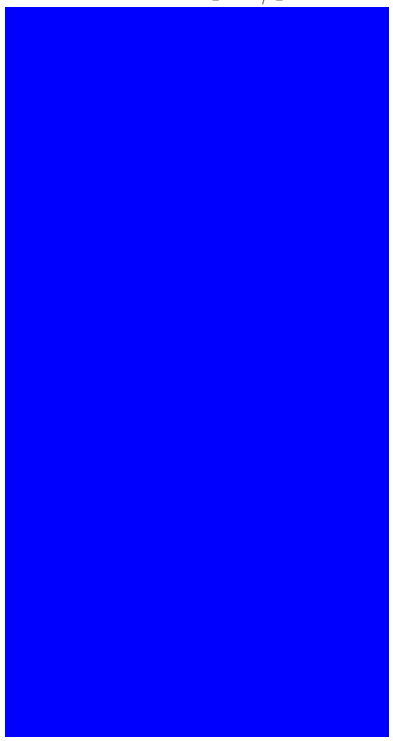

Mode 1 (H_ϕ)

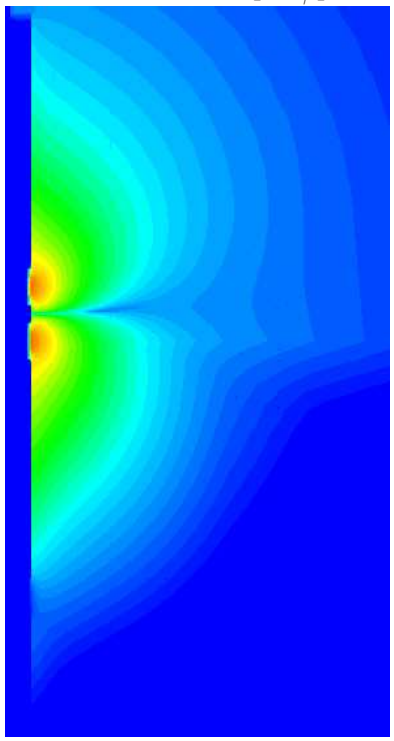

Mode 2 (H_ϕ)

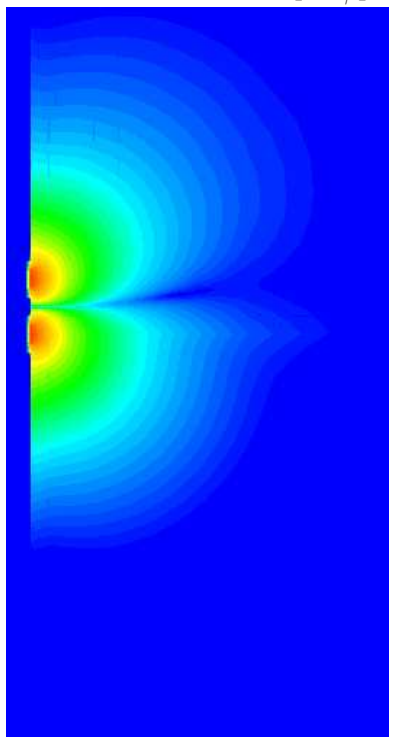

DUAL PROBLEM

EXAMPLE OF 2.5D TRIAXIAL INDUCTION LWD PROBLEM

TRIAXIAL INDUCTION

2.5D Problem (Triaxial Induction). Source: Horizontal Magnetic Dipole

Mode 0 (H_ρ) **Mode 1 (H_ρ)** **Mode 2 (H_ρ)**

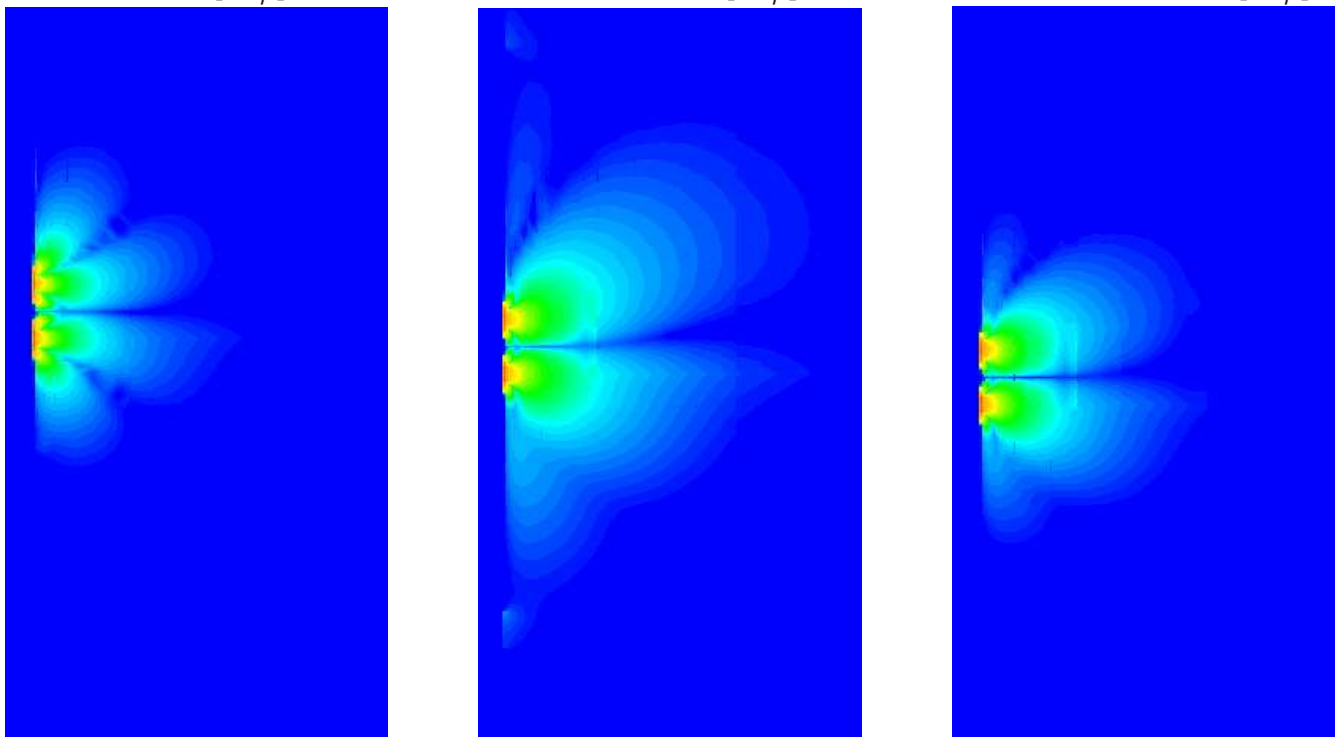

DUAL PROBLEM

EXAMPLE OF 2.5D TRIAXIAL INDUCTION LWD PROBLEM

TRIAXIAL INDUCTION

2.5D Problem (Triaxial Induction). Source: Horizontal Magnetic Dipole

Mode 0 (H_z)

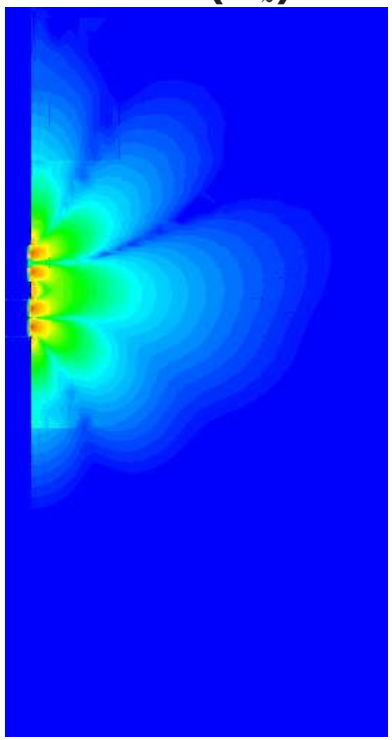

Mode 1 (H_z)

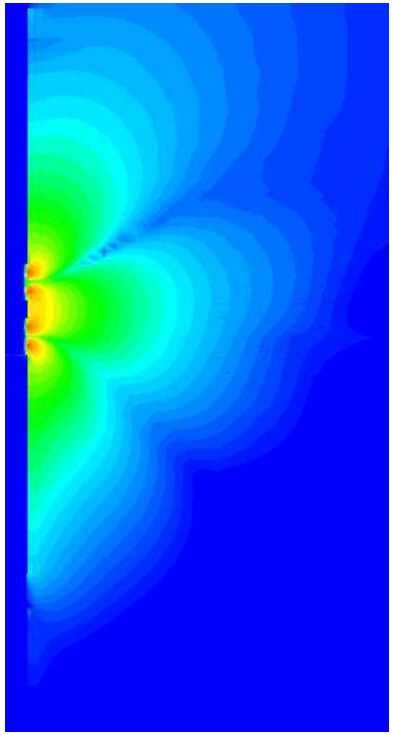

Mode 2 (H_z)

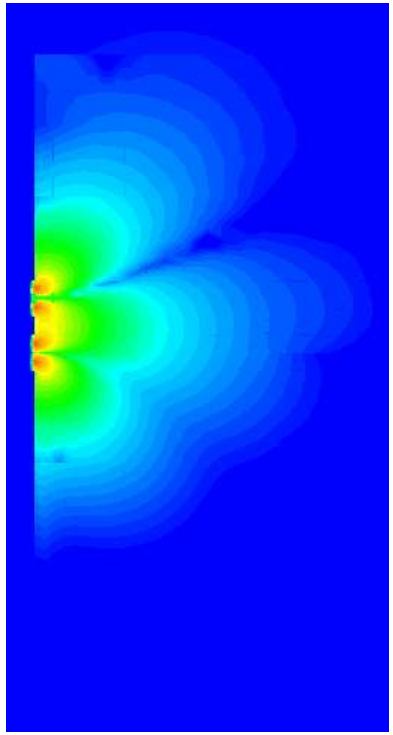

DUAL PROBLEM

EXAMPLE OF 2.5D TRIAXIAL INDUCTION LWD PROBLEM

TRIAXIAL INDUCTION

2.5D Problem (Triaxial Induction). Source: Horizontal Magnetic Dipole

Mode 0 (H_ϕ) **Mode 1 (H_ϕ)** **Mode 2 (H_ϕ)**

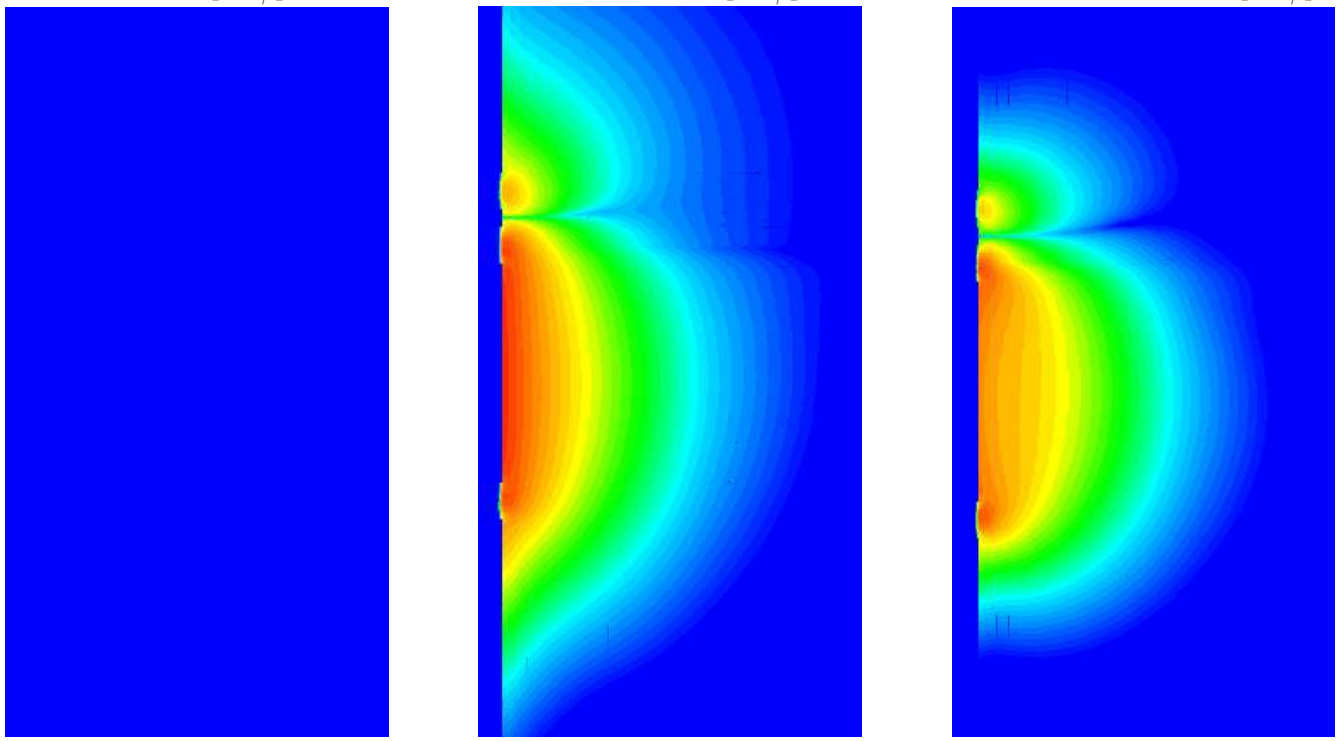

DIRECT SOLUTION TIMES DUAL SOLUTION
EXAMPLE OF 2.5D TRIAXIAL INDUCTION LWD PROBLEM

TRIAXIAL INDUCTION

2.5D Problem (Triaxial Induction). Source: Horizontal Magnetic Dipole

Mode 0 (H_ρ)

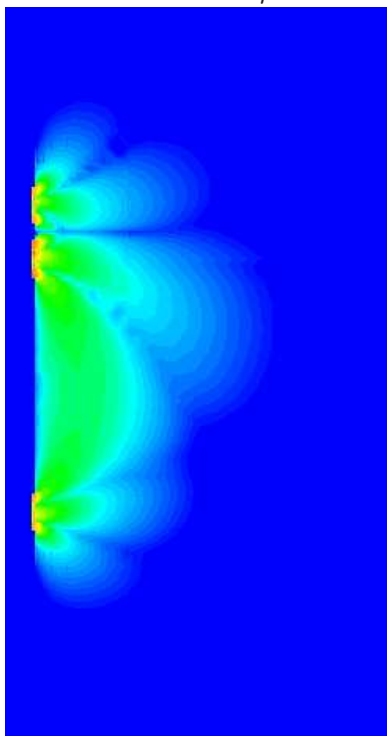

Mode 1 (H_ρ)

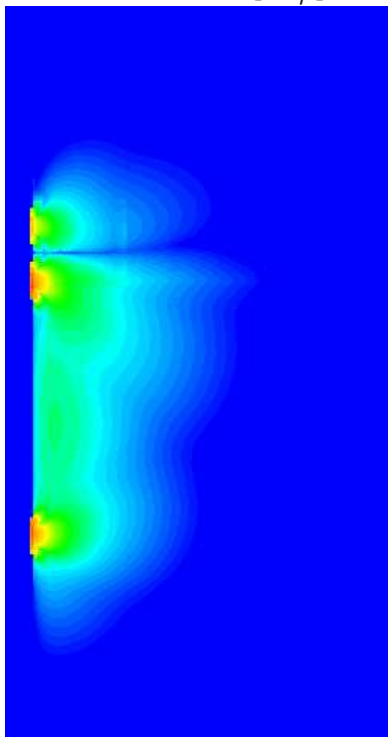

Mode 2 (H_ρ)

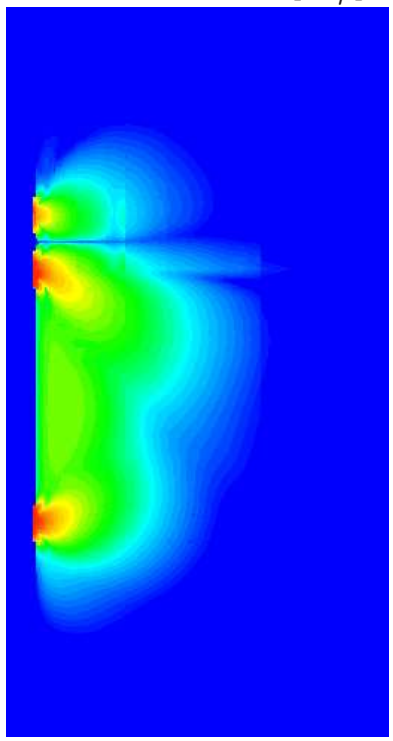

DIRECT SOLUTION TIMES DUAL SOLUTION
EXAMPLE OF 2.5D TRIAXIAL INDUCTION LWD PROBLEM

TRIAXIAL INDUCTION

2.5D Problem (Triaxial Induction). Source: Horizontal Magnetic Dipole

Mode 0 (H_z) **Mode 1 (H_z)** **Mode 2 (H_z)**

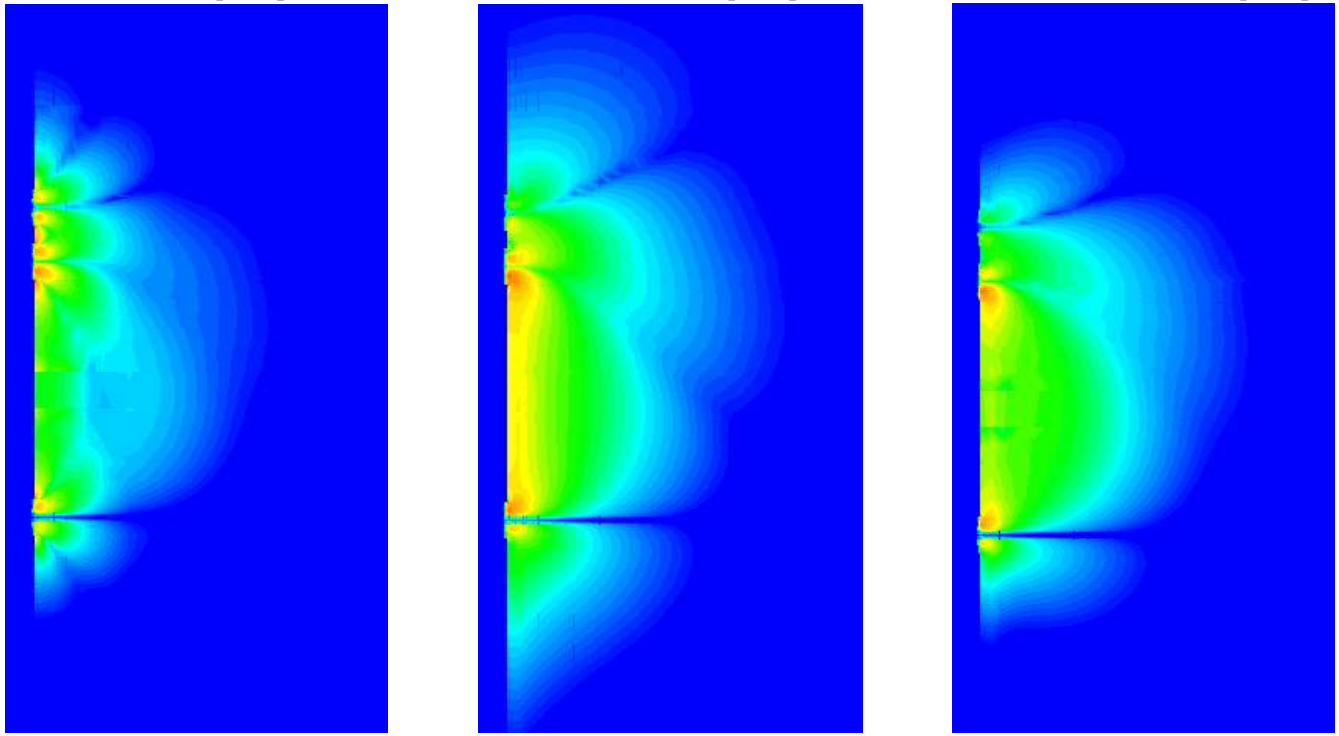

DIRECT SOLUTION TIMES DUAL SOLUTION
EXAMPLE OF 2.5D TRIAXIAL INDUCTION LWD PROBLEM

CONCLUSIONS AND FUTURE WORK

Conclusions

- A Fourier-Finite-Element method combined with a 2D parallel self-adaptive refinament strategy enables efficient and accurate simulations of a large class of geophysical resistivity problems.
- A unique software can be used to study the response of through-casing, dual laterolog, triaxial induction, and logging-while-drilling instruments in possibly deviated wells, in the presence of rugosity, anisotropy, invasion, etc.

Future Work

- Inversion
- Multi-physics
- Marine controlled source EM applications.

ACKNOWLEDGMENTS

Sponsors of UT Austin's consortium on Formation Evaluation